Physical limit of information storage

-The prospect of Spintronics-

Ching-Ray Chang

Center for Nanostorage Research
and
Department of Physics
National Taiwan University

Email: crchang@phys.ntu.edu.tw

Spintronics R&D

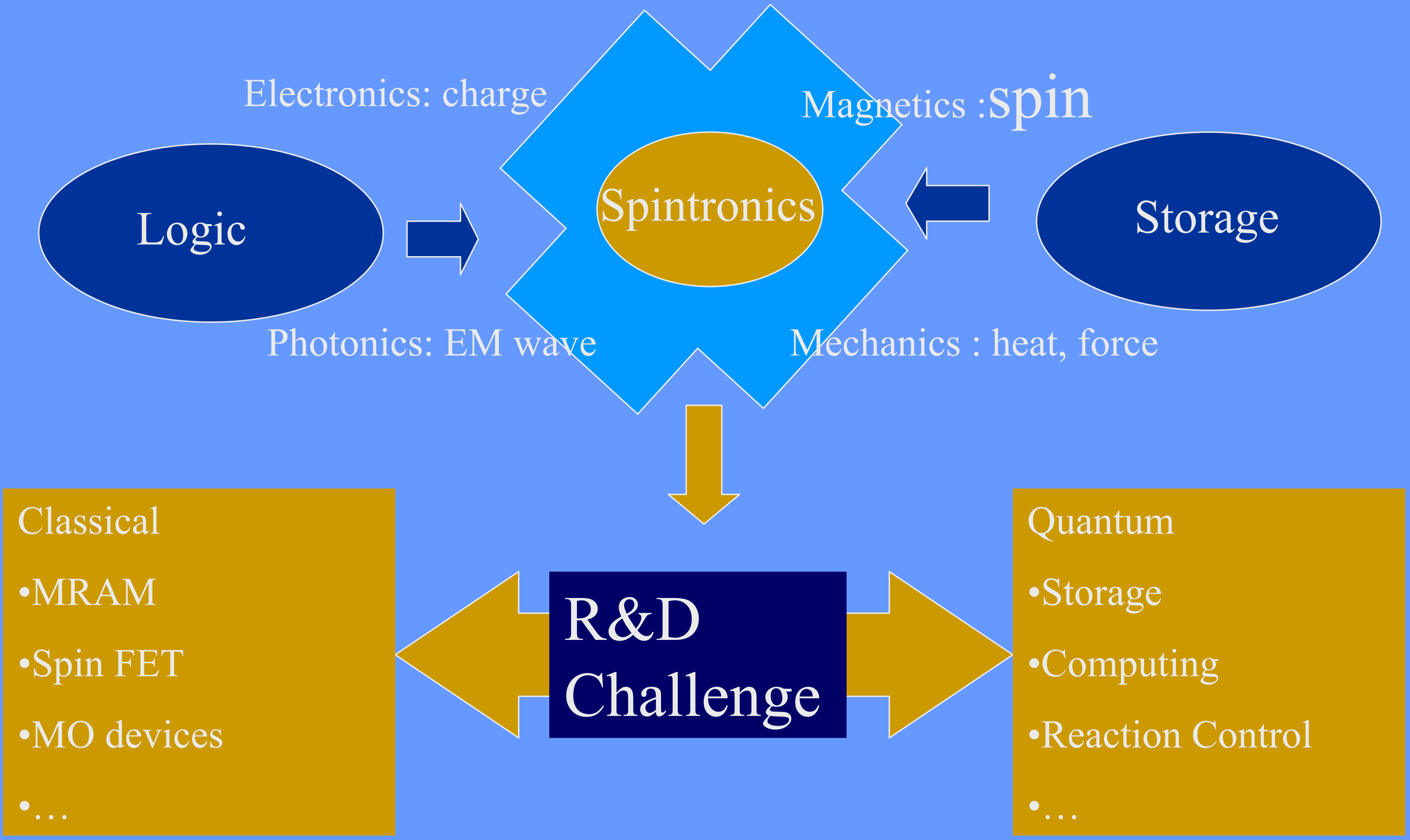

Electronics: charge

Magnetics :spin

Logic

Spintronics

Storage

Photonics: EM wave

Mechanics : heat, force

Classical
- MRAM
- Spin FET
- MO devices
- …

R&D Challenge

Quantum
- Storage
- Computing
- Reaction Control
- …

Exchange splitting of ferromagenet

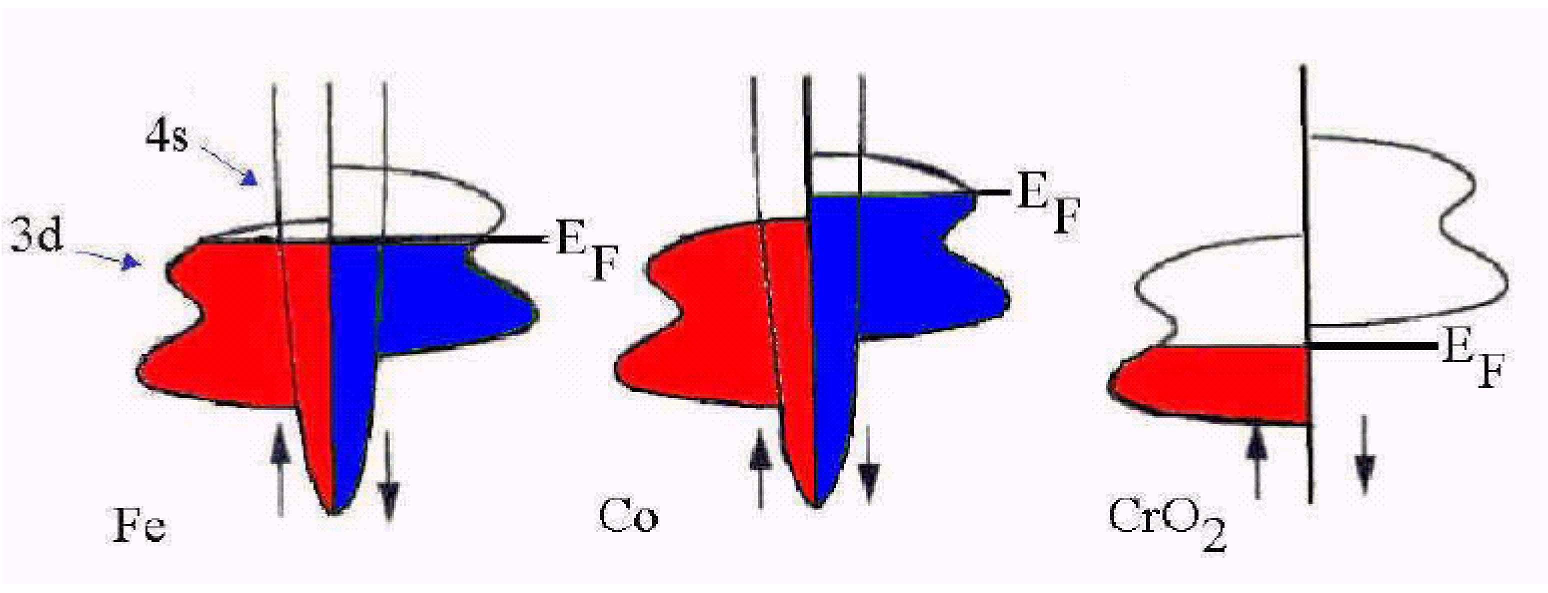

Spintronics

- Spin memory
- Half metal
- Magnetic Spin Semiconductor
- Spin Movement and Injection
- Spin Detection and Spin Transfer
- Spin-Based FET and Transistor
- Spin-Based Computing

Spin valve / MTJ

- Spin valve

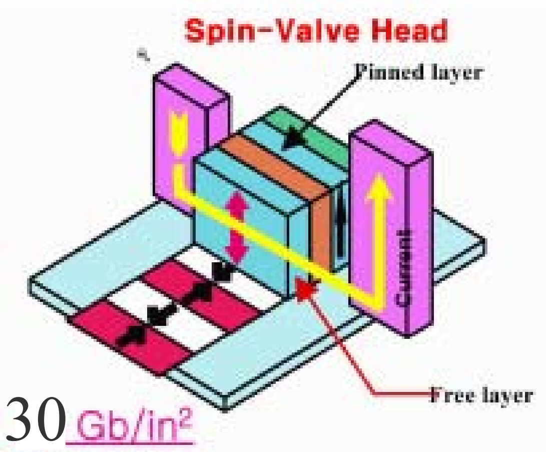

130 Gb/in²

- MTJ

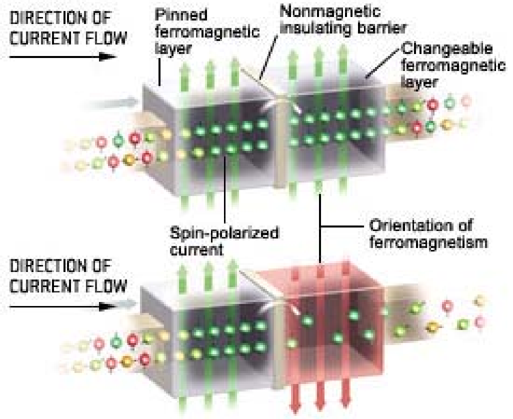

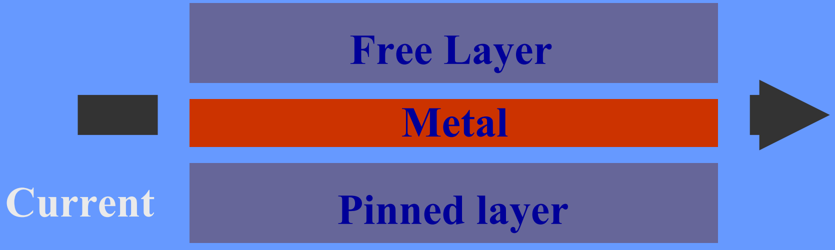

Free Layer

Metal

Pinned layer

Current

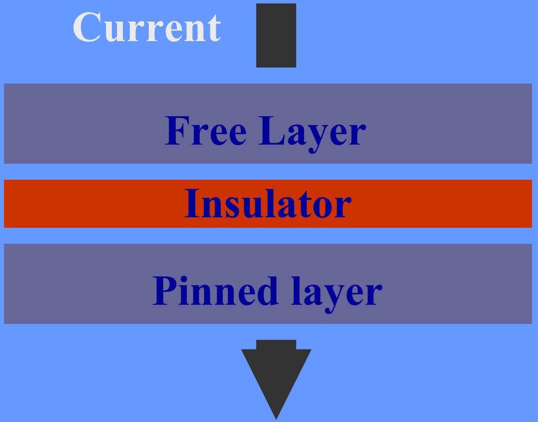

Current

Free Layer

Insulator

Pinned layer

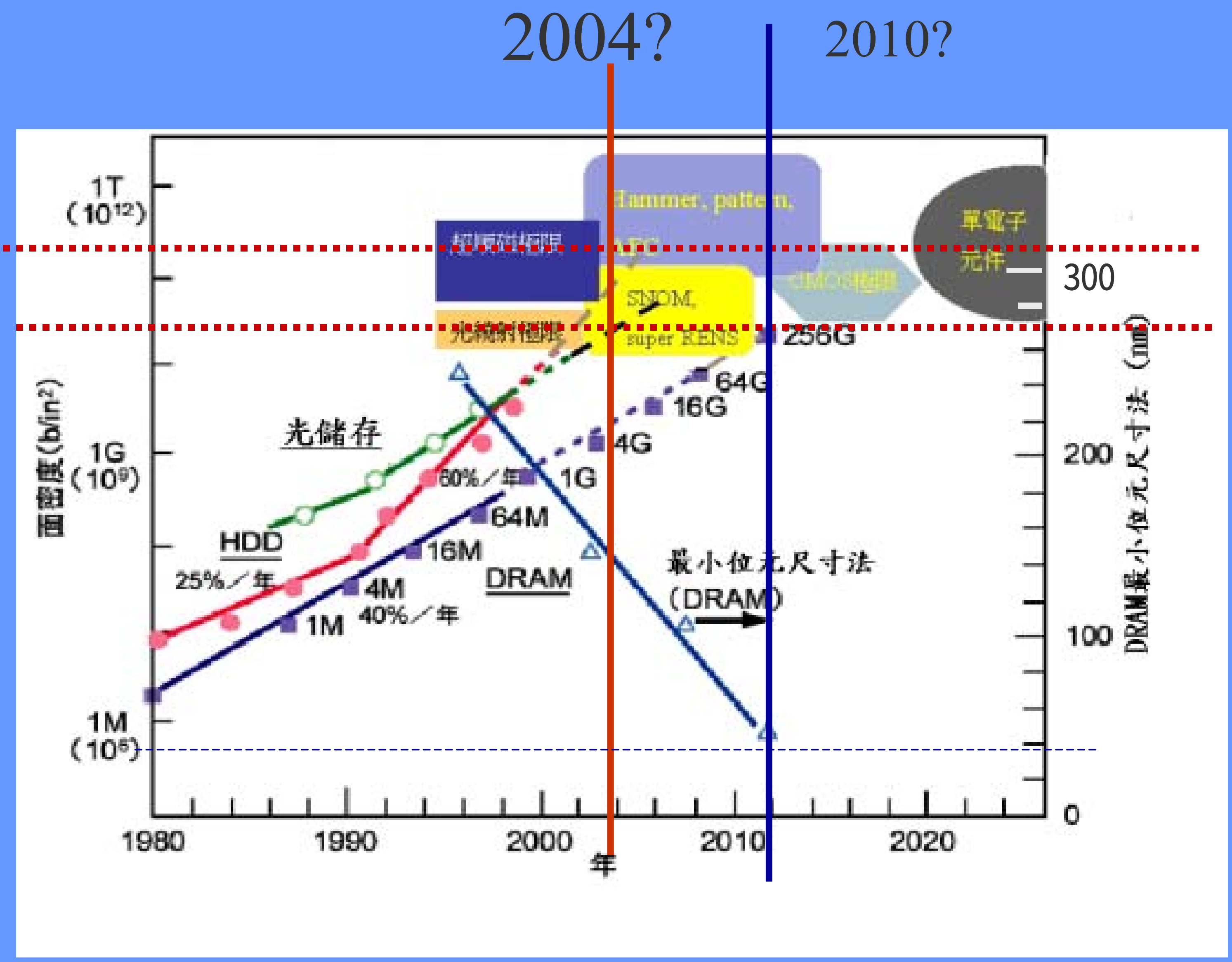2004?
2010?
300
1T
(10¹²)
1G
(10⁹)
1M
(10⁶)
面密度(b/in²)
超順磁極限
光繞射極限
Hammer, pattern,
APC
SNOM,
super RENS
CMOS極限
單電子
元件
256G
64G
16G
4G
1G
64M
16M
4M
1M
光儲存
HDD
25%／年
60%／年
40%／年
DRAM
最小位元尺寸法
(DRAM)
200
100
0
DRAM最小位元尺寸法 (nm)
1980
1990
2000
2010
2020
年

Electrons:

New DOF in
Condensed Matters

- 1897: Thompson : Charge
- 1921: Stern-Gelache : Spin (A beauty only for Physicists, but still a sleeping beauty for the world)
- 1988 : Gruburger, Fert (Prince kiss the Sleeping Beauty and wake her up to the world)

1988:nano

1897:macroscopic

Semi-Classic Model of Spin-dependent Transport

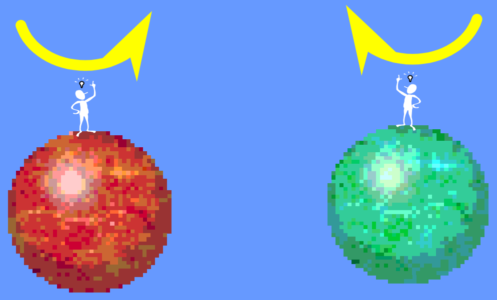

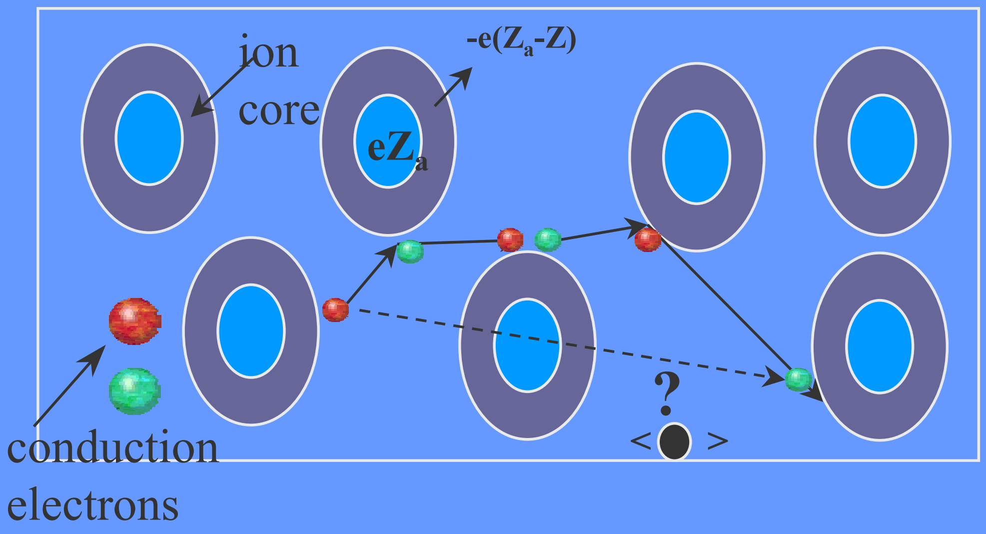

Characteristic Length

- Wavelength :

$$\lambda \approx k_F$$

Carriers ⇨

$$k_F = \frac{3.63}{r_s / a_0} \overset{\circ}{A}{}^{-1} \propto n^{1/3}$$

metal(~10^{22}cm^{-3}): ~ *0.1nm*

semiconductor(< 10^{16}cm^{-3}): > *10nm*

Applications: semiconductor device

- Exchang length :L

Wall width ⇨

$$\sqrt{\frac{A}{K}} \geq 1\ nm$$

Applications: Spintronics

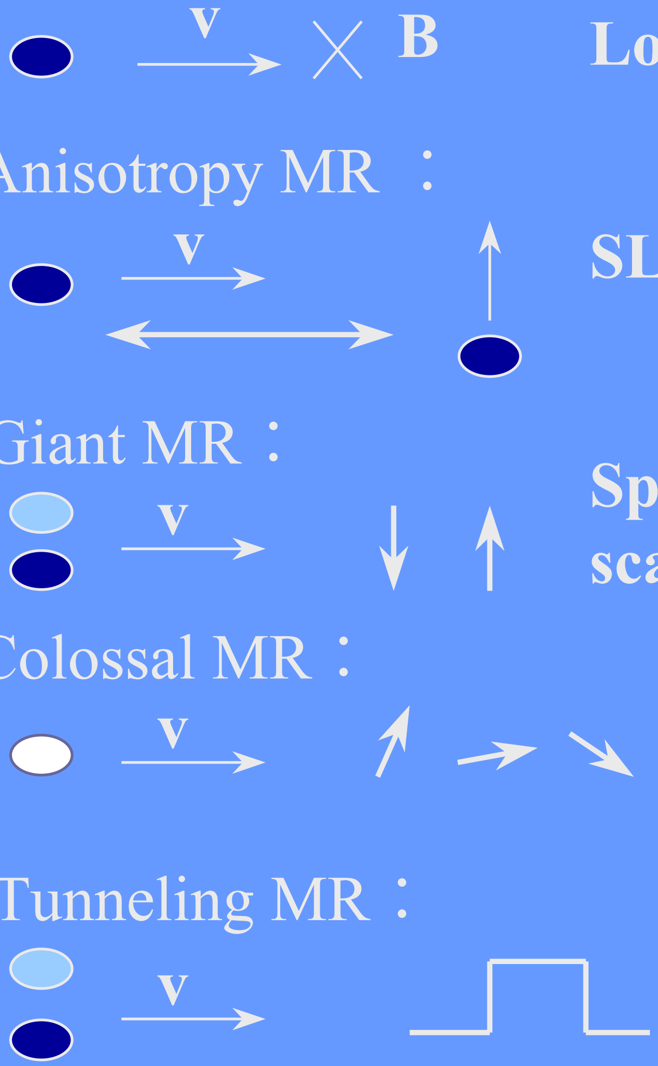

(1) Ordinary MR：

Lorentz Force

(2) Anisotropy MR ：

SL coupling

(3) Giant MR：

Spin dependent scattering

(4) Colossal MR：

LaCaMnO

(5) Tunneling MR：

Insulating Barrier

(6) Polarized 2DEG：

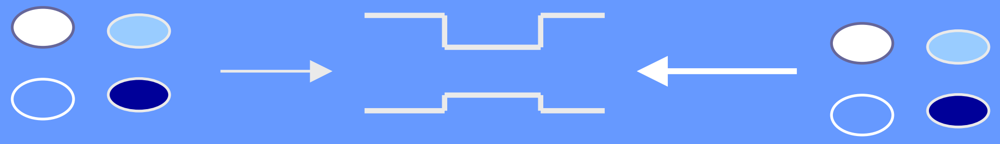

(7) Ferromagnet/Superconductor：

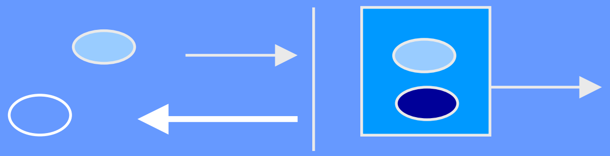

Effective mass? Band? Interference?

Mean-free path? Spin-diffusion length?

Current Memory Hierarchy

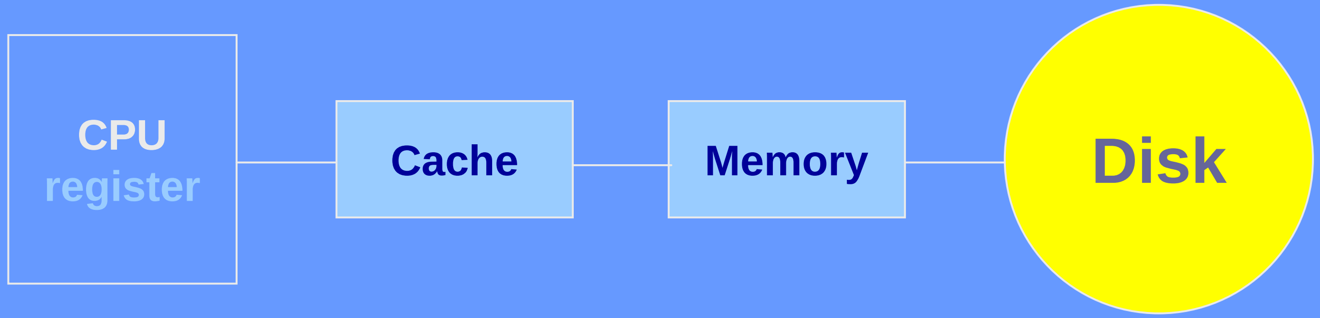

	Register	Cache (SRAM)	Memory (DRAM)	Disk Memory
size:	**200 Bytes**	**32KB/4MB**	**128MB/512MB**	**4GB/20GB**
speed:	**3ns**	**6ns**	**60ns**	**8 ms**
$/MB:		**$1.5**	**$0.015-0.02**	**$0.0015**

Larger, slower, cheaper →

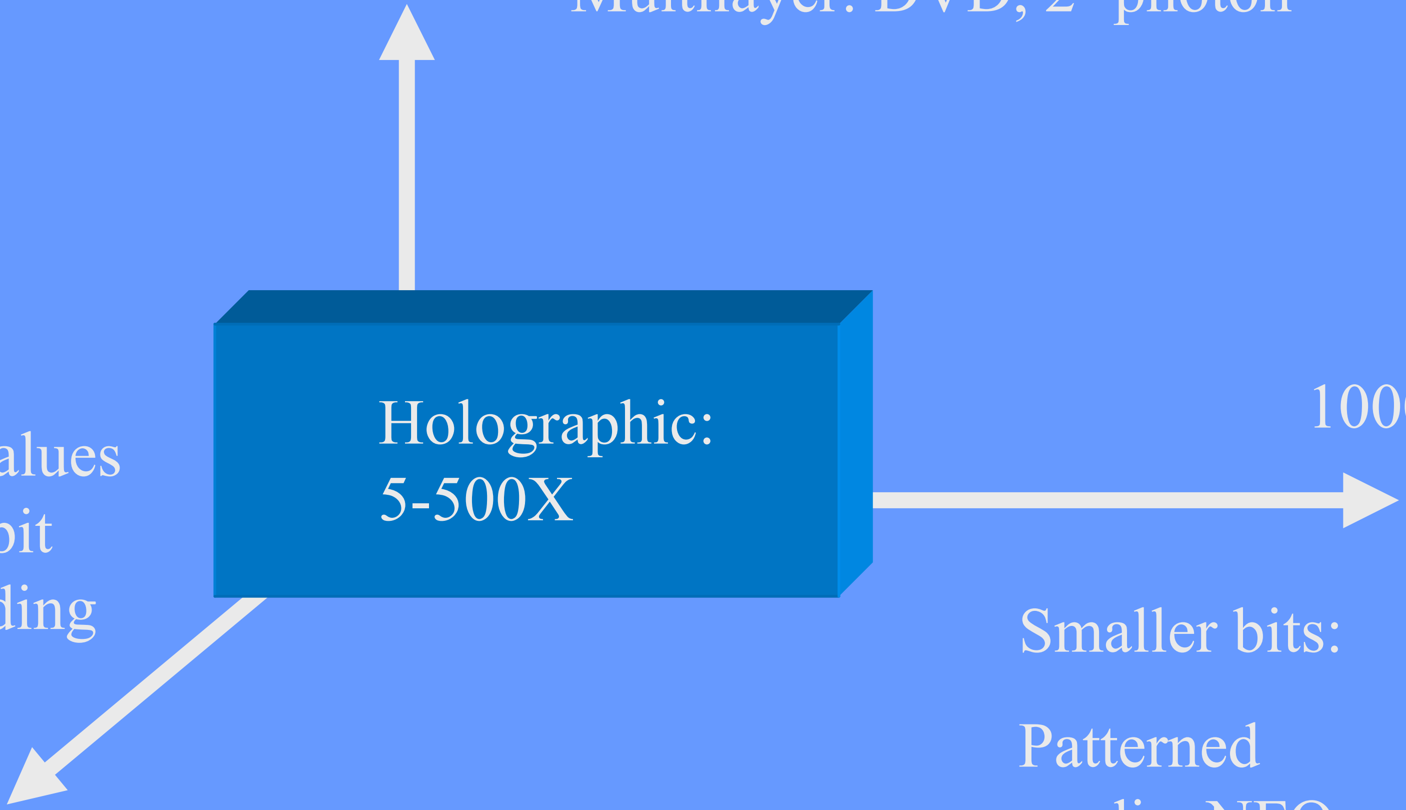

500X

Multilayer: DVD, 2- photon

Multiple values
per mark: pit
depth rcording

Holographic:
5-500X

1000X

Smaller bits:

Patterned
media, NFO,
probe, etc

4X

磁儲存的發展歷史

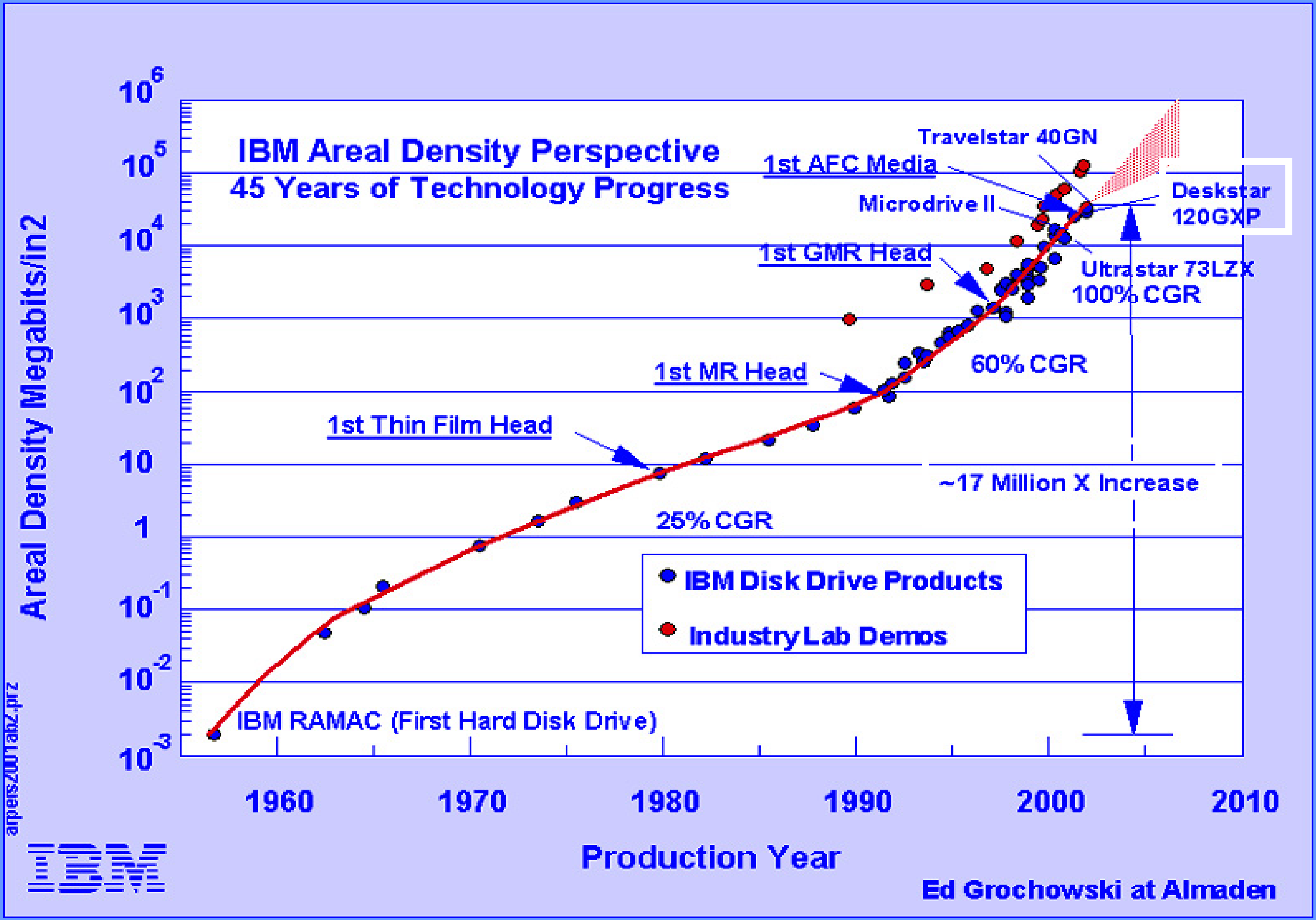
IBM Areal Density Perspective
45 Years of Technology Progress
Areal Density Megabits/in2
10^6
10^5
10^4
10^3
10^2
10
1
10^{-1}
10^{-2}
10^{-3}
1960
1970
1980
1990
2000
2010
Production Year
Travelstar 40GN
1st AFC Media
Microdrive II
Deskstar 120GXP
1st GMR Head
Ultrastar 73LZX
100% CGR
60% CGR
1st MR Head
1st Thin Film Head
~17 Million X Increase
25% CGR
● IBM Disk Drive Products
● Industry Lab Demos
IBM RAMAC (First Hard Disk Drive)
apers2001ab2.prz
IBM
Ed Grochowski at Almaden

Physical limit:

Magnetic : superparamagnetic : Thermal

Optic : Diffraction : wavelength

Semiconductor : optic, carrier number, heat. etc

Shannon Limit: access, Transfer

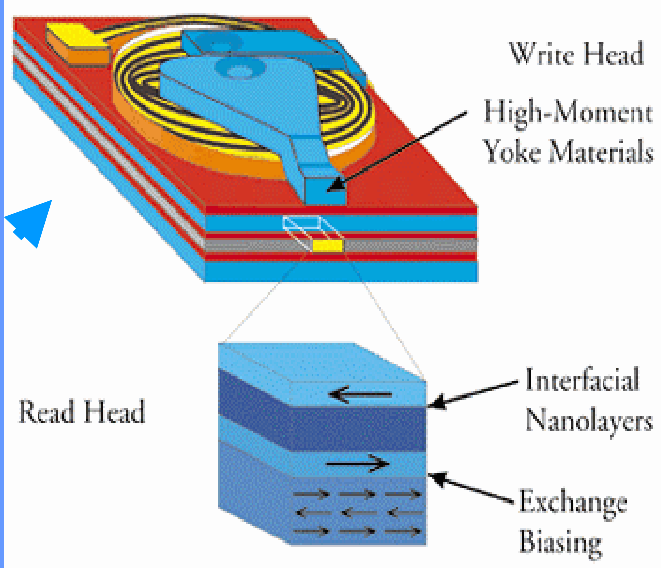

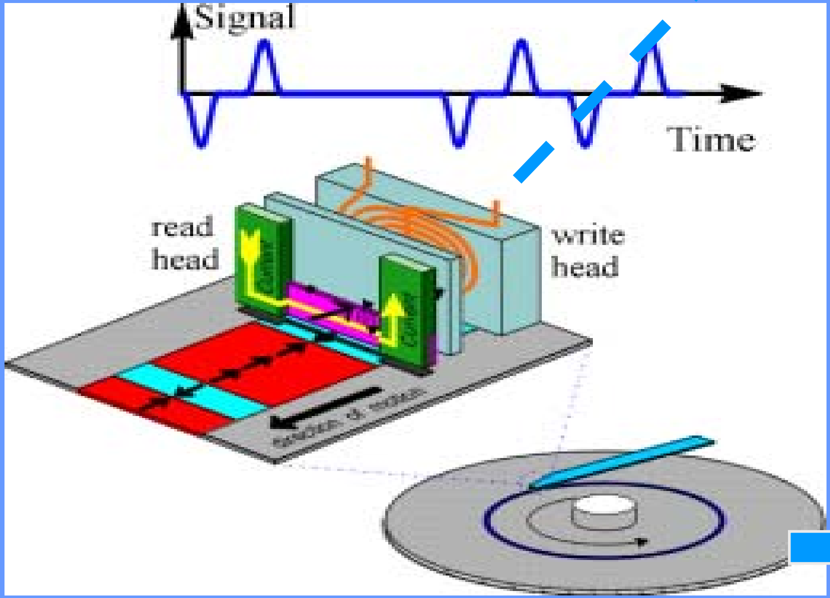

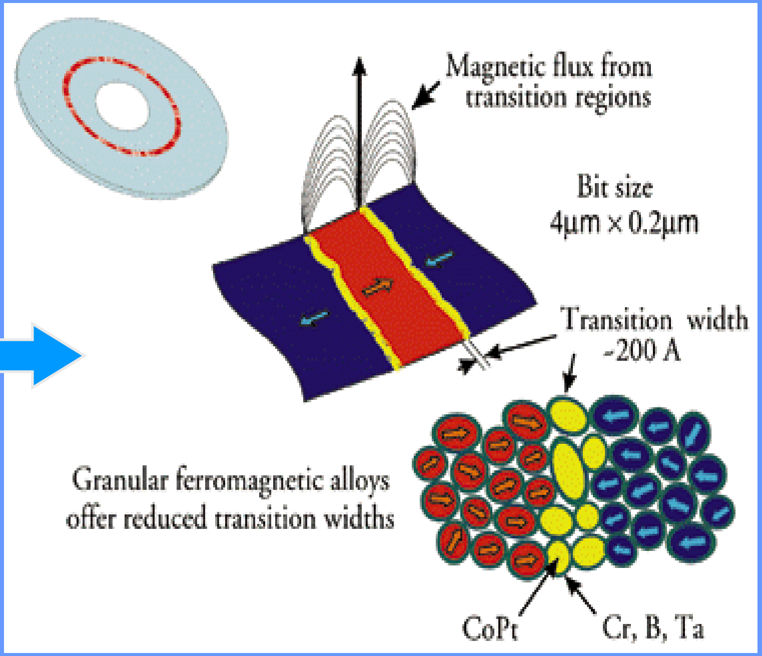

Extracted from www-als.lbl-gov/als/workshops/scidirecthtml/4Magnetic/magnetic.html

GMR示意圖

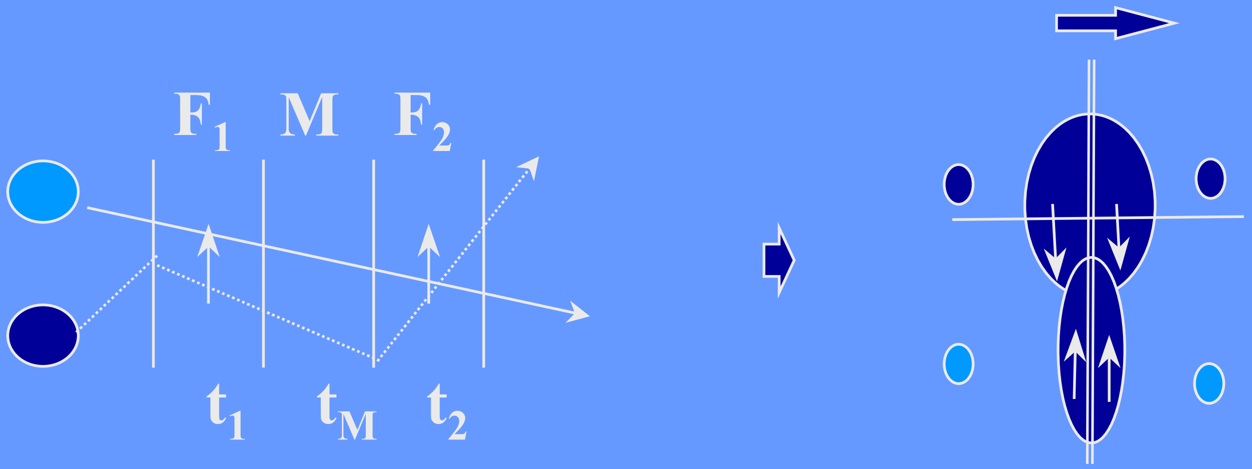

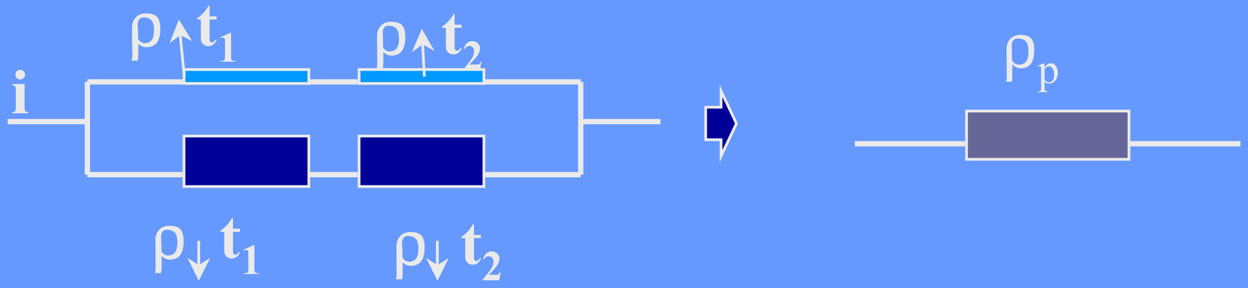

$H = H_S$ ： Parallel ；$t_1=t_2=t/2$

$$\rho_p = (\rho_\uparrow \rho_\downarrow)/(\rho_\uparrow + \rho_\downarrow)$$

GMR示意圖

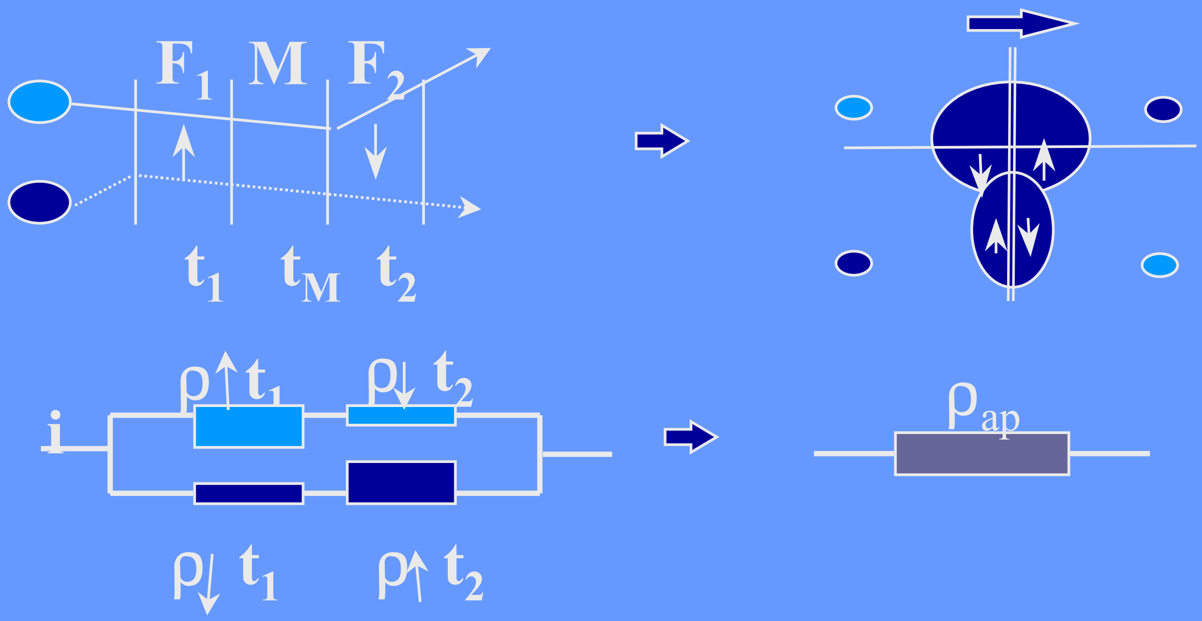

H = 0：Antiparallel; $t_1=t_2=t/2$

$$\rho_{ap} = (\rho_\uparrow + \rho_\downarrow)/4$$

$$\Delta\rho/\rho_{ap} = (\rho_\uparrow - \rho_\downarrow)^2/(\rho_\uparrow + \rho_\downarrow)^2$$

Spinvalve: Exchange Bias

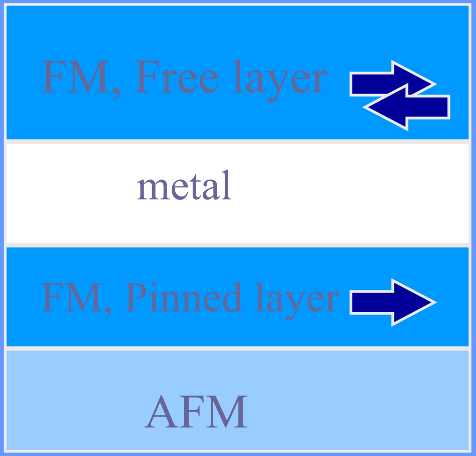

FM, Free layer

metal

FM, Pinned layer

AFM

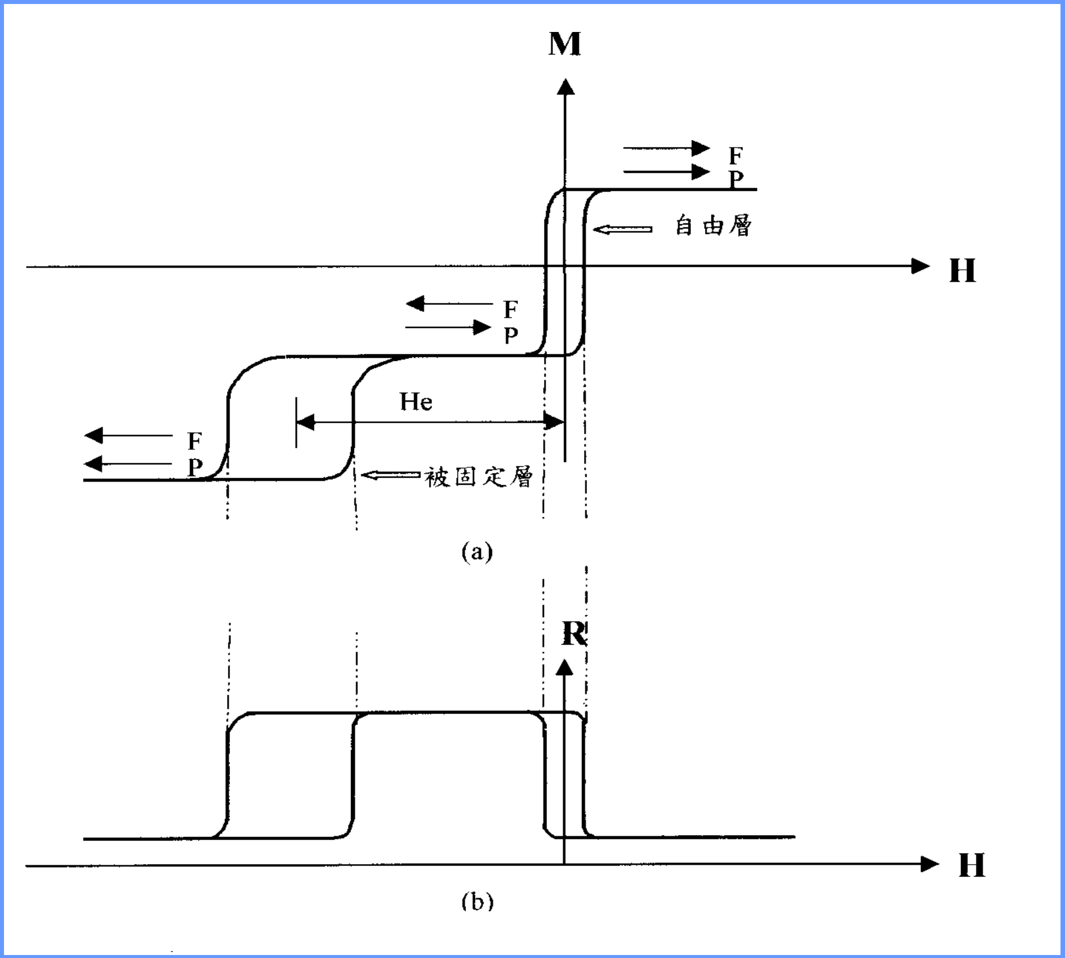

Recent results of Spintronics in NTU

Spintronics Group

New Materails and TMR devices

Prof. JH Hsu, Prof. MT Lin, Prof. JG Lin, Prof. RS Liu

Nano patterned magnetic materials and theoretical simulations

Prof. CR Chang, Prof. J. C. Wu

DMS and functional devices

Prof. YH Chang, Prof. CD Liang

Prof. SC Lee

Experimental Procedure for Co/NiMn Exchange Bias

- e-beam evaporation
- NiMn growth T :
  T > 120 ºC ⇒ epitaxial (001)NiMn
- No applied field
- post-annealing : 280 ºC, 1000 Oe
- XRD & TEM : crystal structure
- VSM & MOKE : hysteresis loops

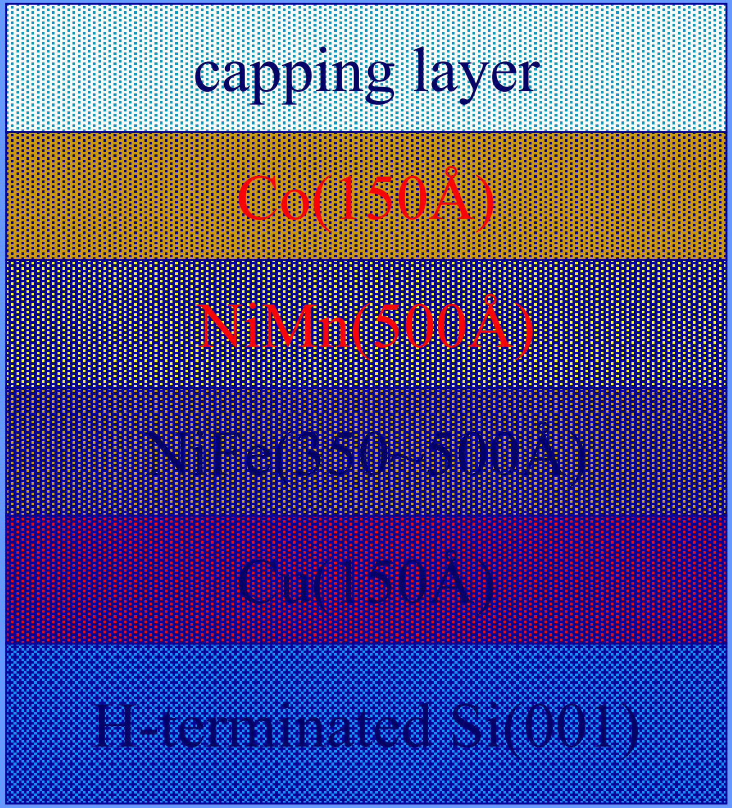

capping layer

Co(150Å)

NiMn(500Å)

NiFe(350-500Å)

Cu(150Å)

H-terminated Si(001)

Surface-induced Biquadratic coupling and the Associated Modified Astroids

PHYSICAL REVIEW B, VOLUME 64, 094420

Exchange-bias-induced double-shifted magnetization curves in Co biaxial films

Chih-Huang Lai and Yung-Hung Wang
Department of Materials Science & Engineering, National Tsing Hua University, HsinChu, Taiwan

Ching-Ray Chang
Department of Physics, National Taiwan University, Taipei, Taiwan

Jyh-Shinn Yang
Institute of Optoelectronic Sciences, National Taiwan Ocean University, Keelung, Taiwan

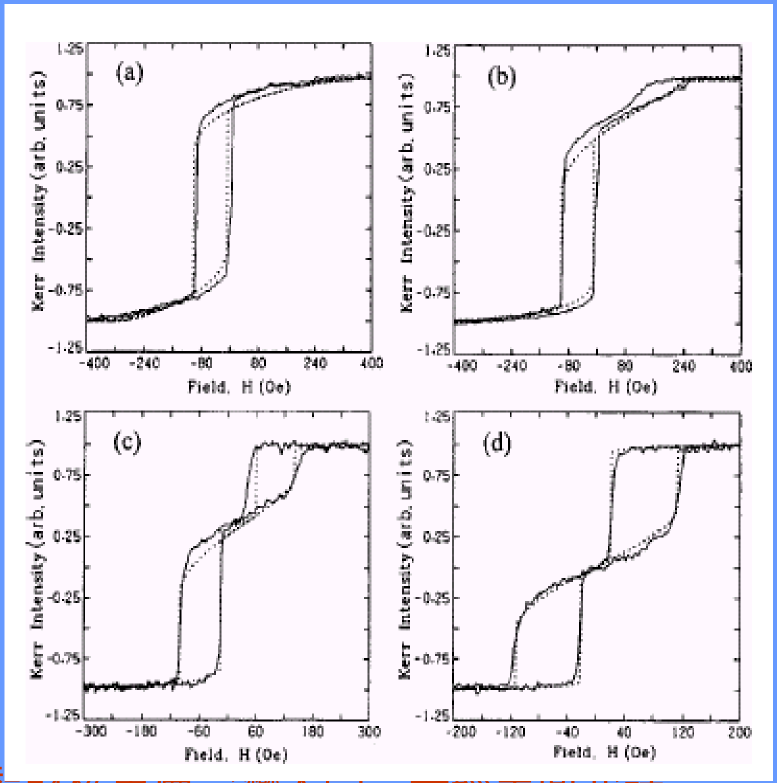

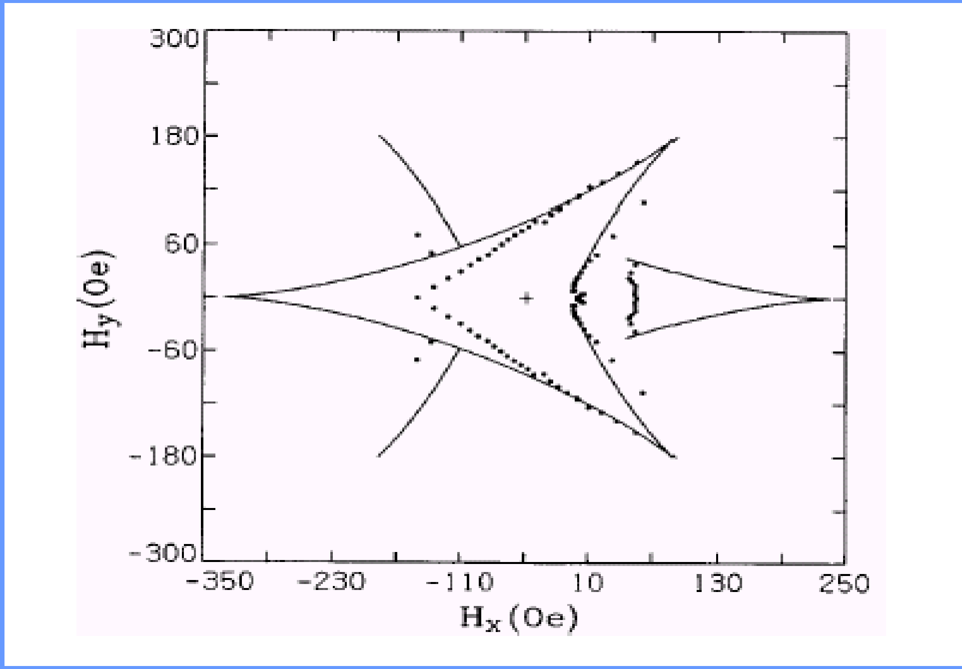

Temperature dependence of long range exchange bias

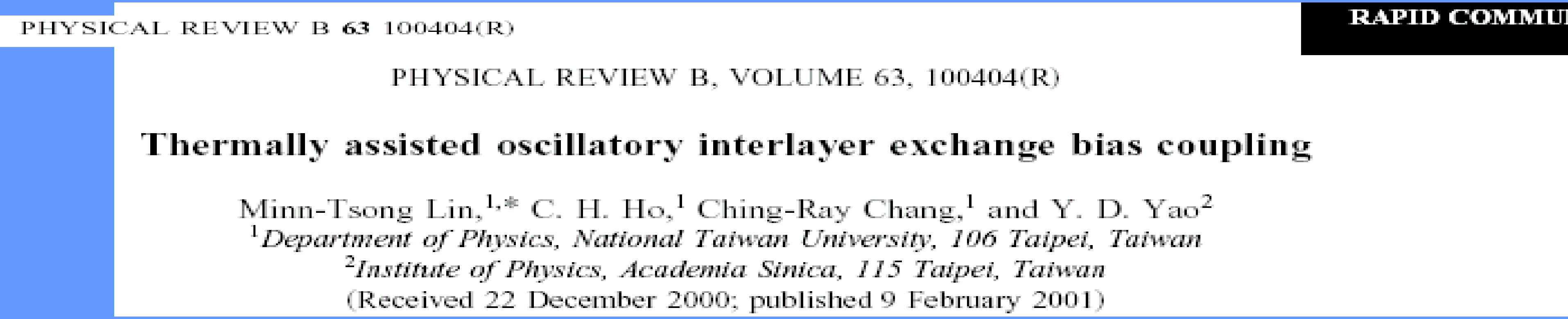

PHYSICAL REVIEW B 63 100404(R)

RAPID COMMU

PHYSICAL REVIEW B, VOLUME 63, 100404(R)

Thermally assisted oscillatory interlayer exchange bias coupling

Minn-Tsong Lin,[1,*] C. H. Ho,[1] Ching-Ray Chang,[1] and Y. D. Yao[2]
[1]*Department of Physics, National Taiwan University, 106 Taipei, Taiwan*
[2]*Institute of Physics, Academia Sinica, 115 Taipei, Taiwan*

(Received 22 December 2000; published 9 February 2001)

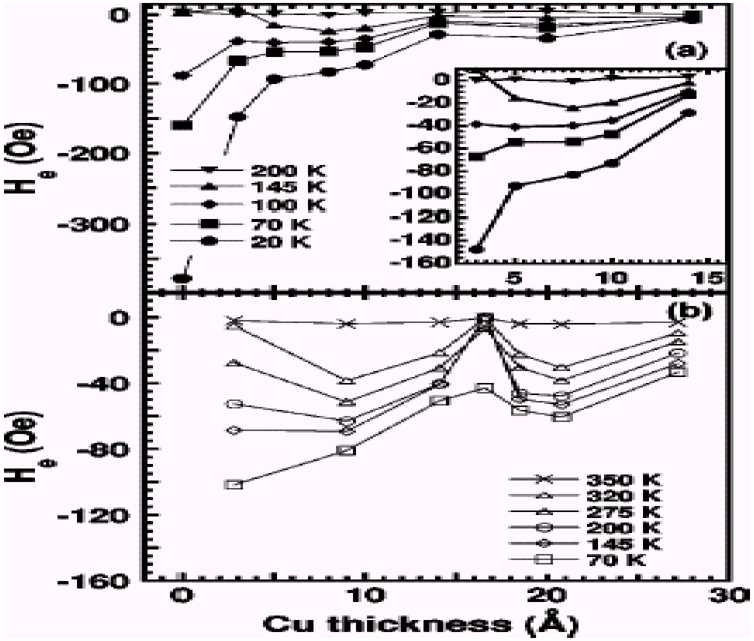

NiFe(100Å):FM
Cu(t Å):Metal
NiO(100Å):AF

$$E_b = J_{inter}(T,d) S_{FM} S_{AF,i} + J_{AF}(T) S_{AF,i} S_{AF}, \qquad (1)$$

Dipolar + RKKY

Highly-uncompensated-spin Interface

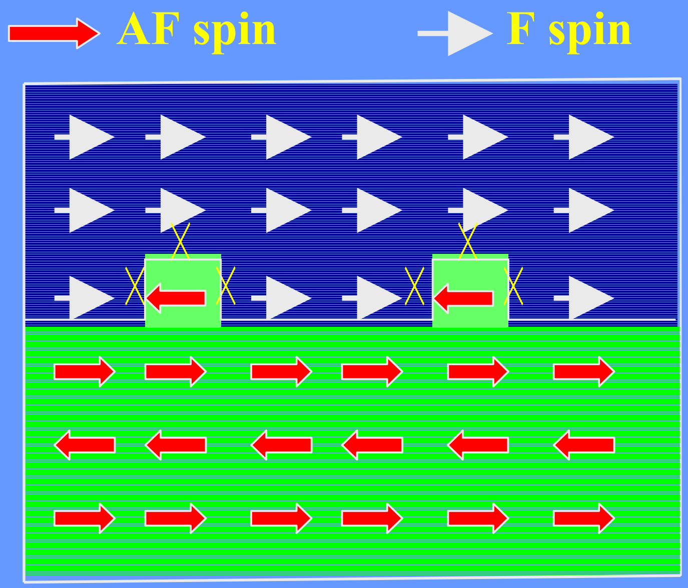

Pinned layer

interface

Pinning layer

⇨ **Highly-uncompensated-spin interface exists in bilayers.**

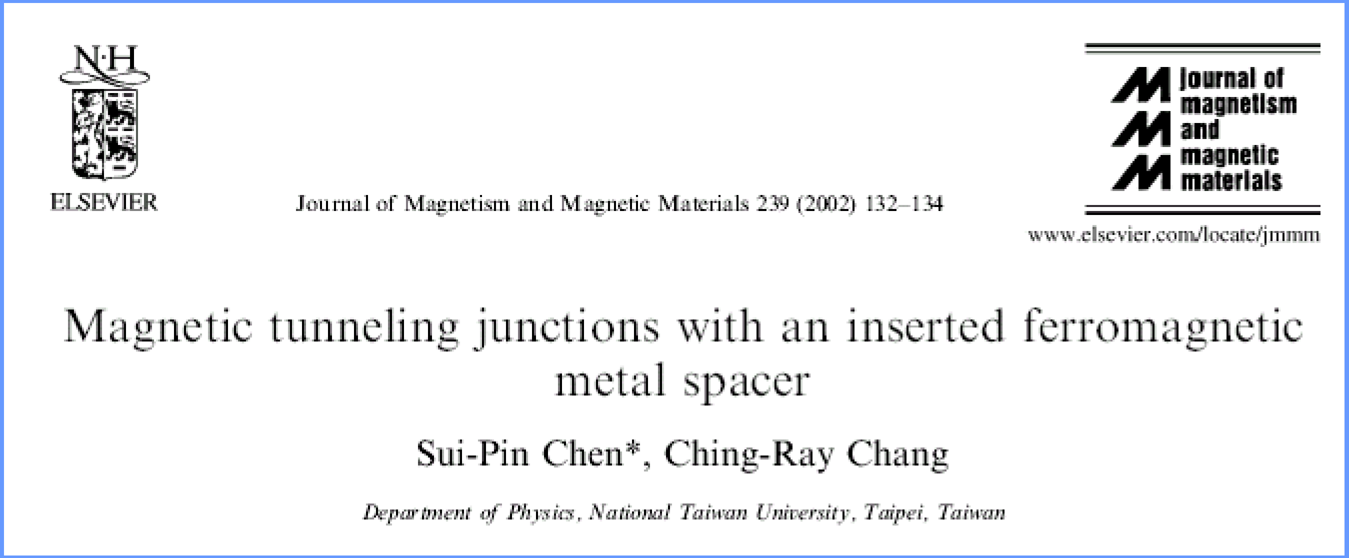

ELSEVIER

Journal of Magnetism and Magnetic Materials 239 (2002) 132–134

journal of magnetism and magnetic materials

www.elsevier.com/locate/jmmm

Magnetic tunneling junctions with an inserted ferromagnetic metal spacer

Sui-Pin Chen*, Ching-Ray Chang

Department of Physics, National Taiwan University, Taipei, Taiwan

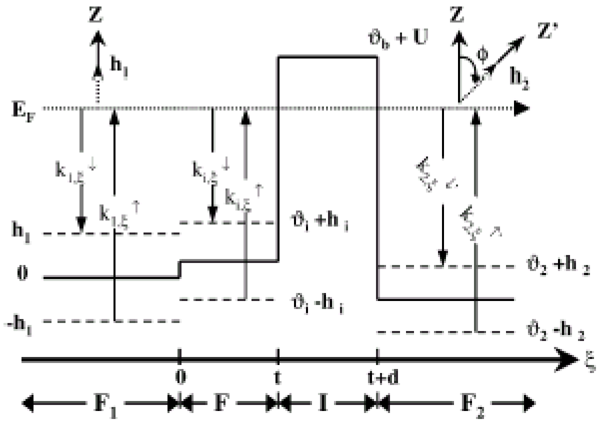

Fig. 1. Schematic diagram for an F_1–F–I–F_2 tunneling junction.

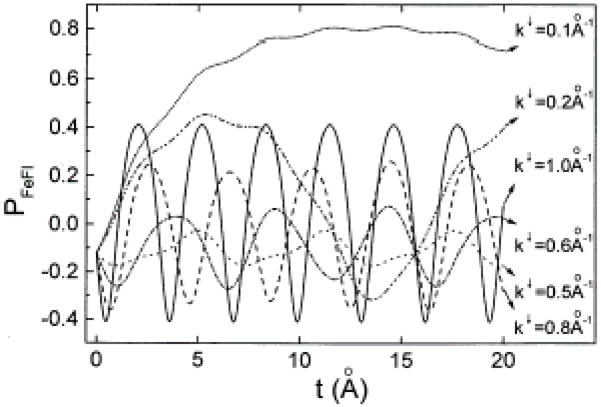

Fig. 2. The effective spin polarization of the Fe–F–I region in an Fe–F–I–F_2 junction versus the thickness *t* of the ferromagnetic spacer.

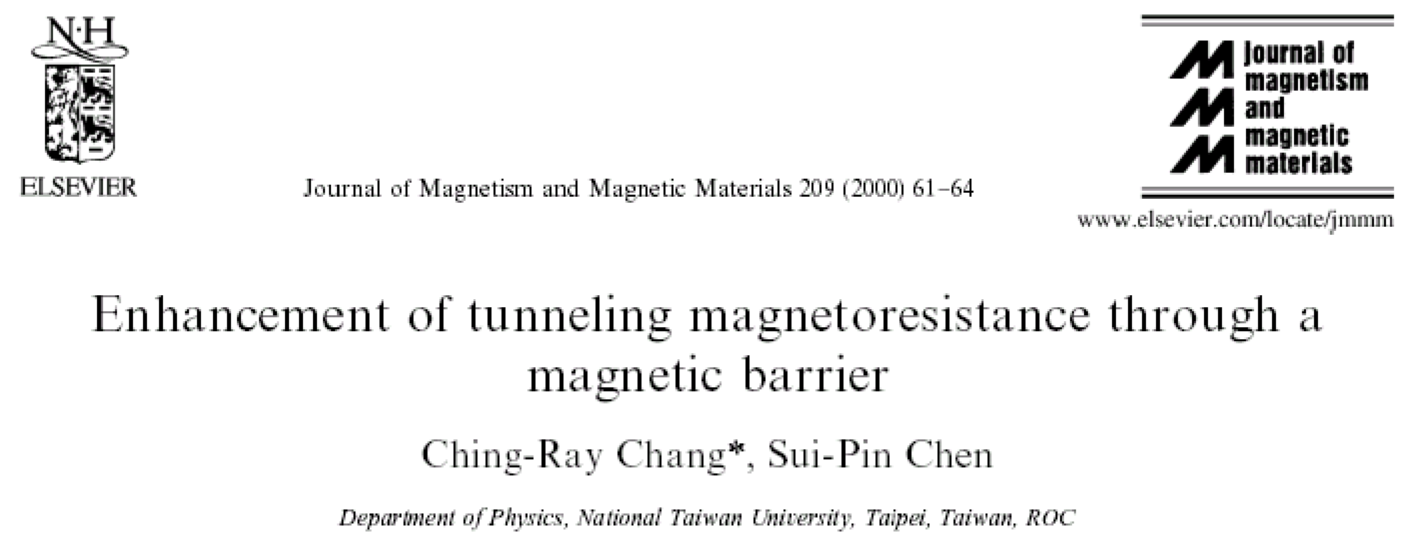

ELSEVIER

Journal of Magnetism and Magnetic Materials 209 (2000) 61–64

journal of magnetism and magnetic materials

www.elsevier.com/locate/jmmm

Enhancement of tunneling magnetoresistance through a magnetic barrier

Ching-Ray Chang*, Sui-Pin Chen

Department of Physics, National Taiwan University, Taipei, Taiwan, ROC

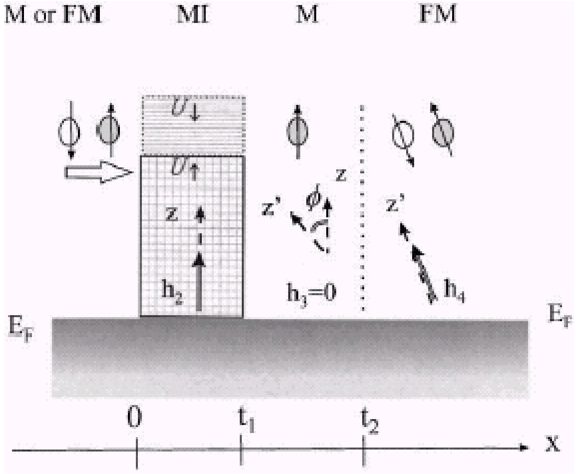

Fig. 1. Schematic diagram for an FM–MI–M–FM tunneling junction. The molecular field h_i is along their spin quantization axis and the angle between z and z' is ϕ.

$$\frac{\Delta R}{R}=\frac{2P_{\mathrm{eff}}}{1+P_{\mathrm{eff}}}.$$

JOURNAL OF APPLIED PHYSICS VOLUME 90, NUMBER 12 15 DECEMBER 2001

Magnetoresistance of spin-dependent tunnel junctions with composite electrodes

C. H. Ho and Minn-Tsong Lin[a)]
Department of Physics, National Taiwan University, 106 Taipei, Taiwan

Y. D. Yao and S. F. Lee
Institute of Physics, Academia Sinica, 115 Taipei, Taiwan

C. C. Liao, F. R. Chen, and J. J. Kai
Department of Engineering and System Science, National Tsing-Hua University, 300 Hsinchu, Taiwan

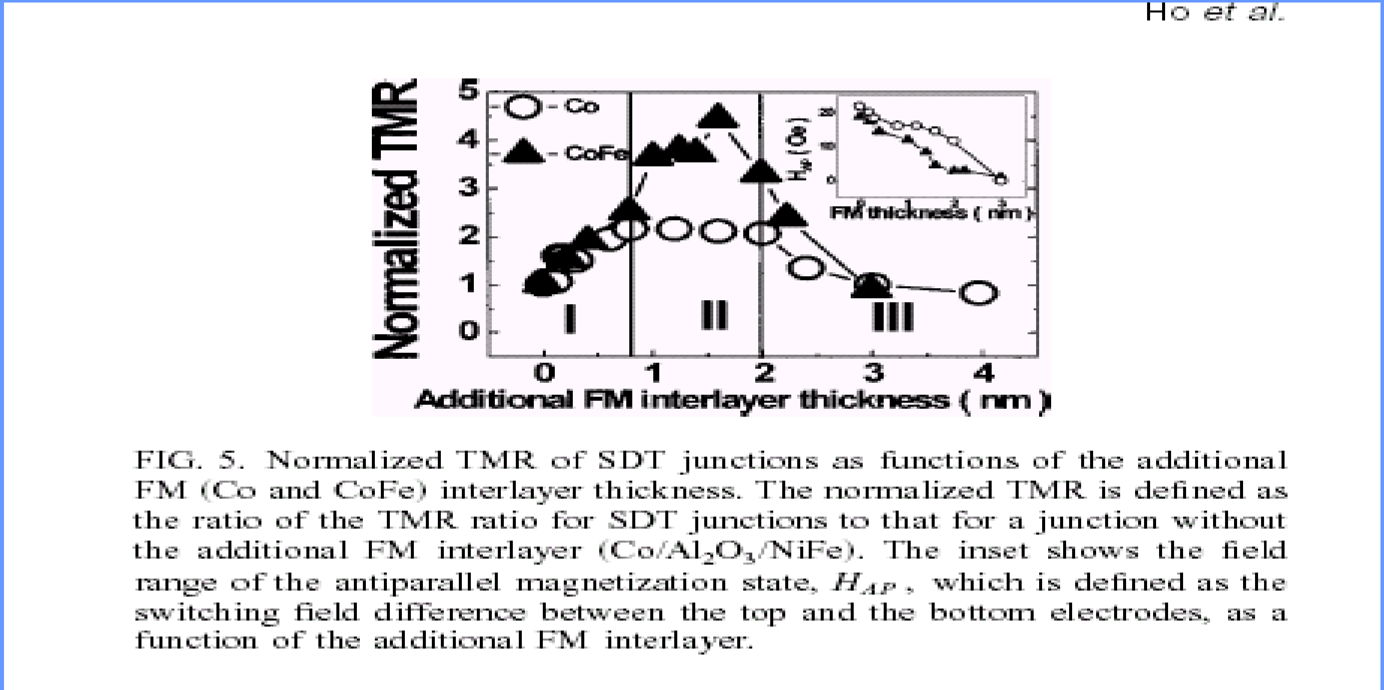

Ho *et al.*

FIG. 5. Normalized TMR of SDT junctions as functions of the additional FM (Co and CoFe) interlayer thickness. The normalized TMR is defined as the ratio of the TMR ratio for SDT junctions to that for a junction without the additional FM interlayer ($Co/Al_2O_3/NiFe$). The inset shows the field range of the antiparallel magnetization state, H_{AP}, which is defined as the switching field difference between the top and the bottom electrodes, as a function of the additional FM interlayer.

Magneto-transport behavior of Half-Metallic Fe3O4

Features of half-metallic magnetite

1) Ferrite
2) Conventional magnetic recording medium material
3) Structure :
4) Electrical:
5) Magnetic:
6) Surface states:
7) Spin Polarization:
8) Electronic Band structures:

Insulator(絕緣體)

Semi-conductor(半導體)

Semi-metal(半金屬)　(準金屬)

Half-metallic(?金屬)　(半金屬or 單自旋金屬)

Metal(金屬)

Super-conductor(超導體)

Our Sputtering System:

(a) 直流磁旋濺鍍法

(b) 基版:Si(100)

(c) 基版溫度:300^{o}C

(d) 濺鍍前壓力:2x10^{-6}torr

(e) 濺鍍工作壓力:5mTorr

(f) 濺鍍時電流:100mA

(g) 薄膜厚度:100nm~500nm

Unique point: low thermal conditions

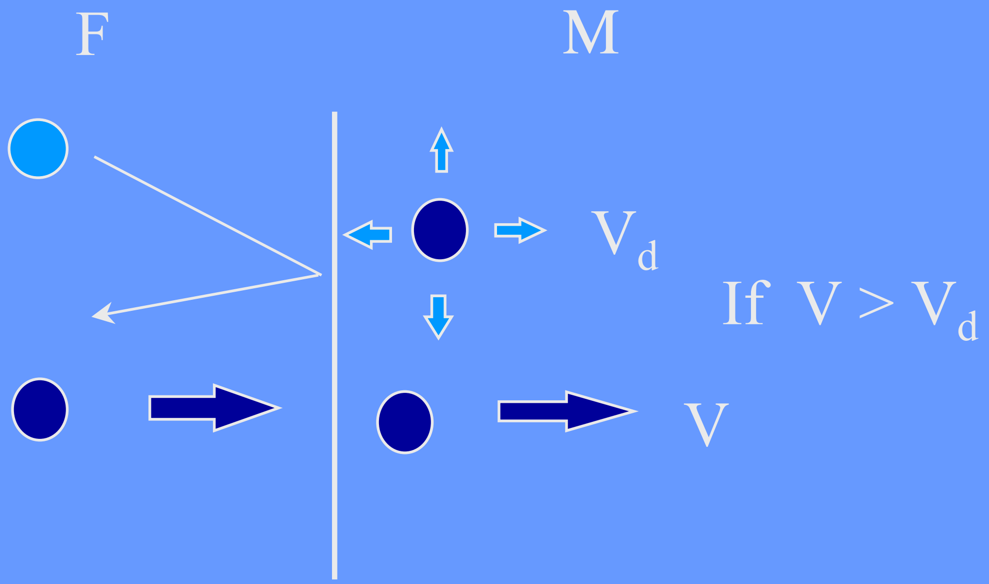

Spin Accumulation

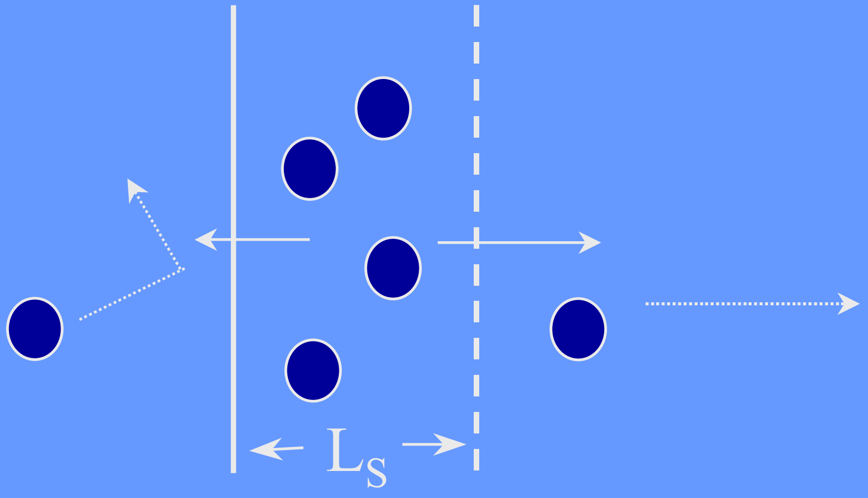

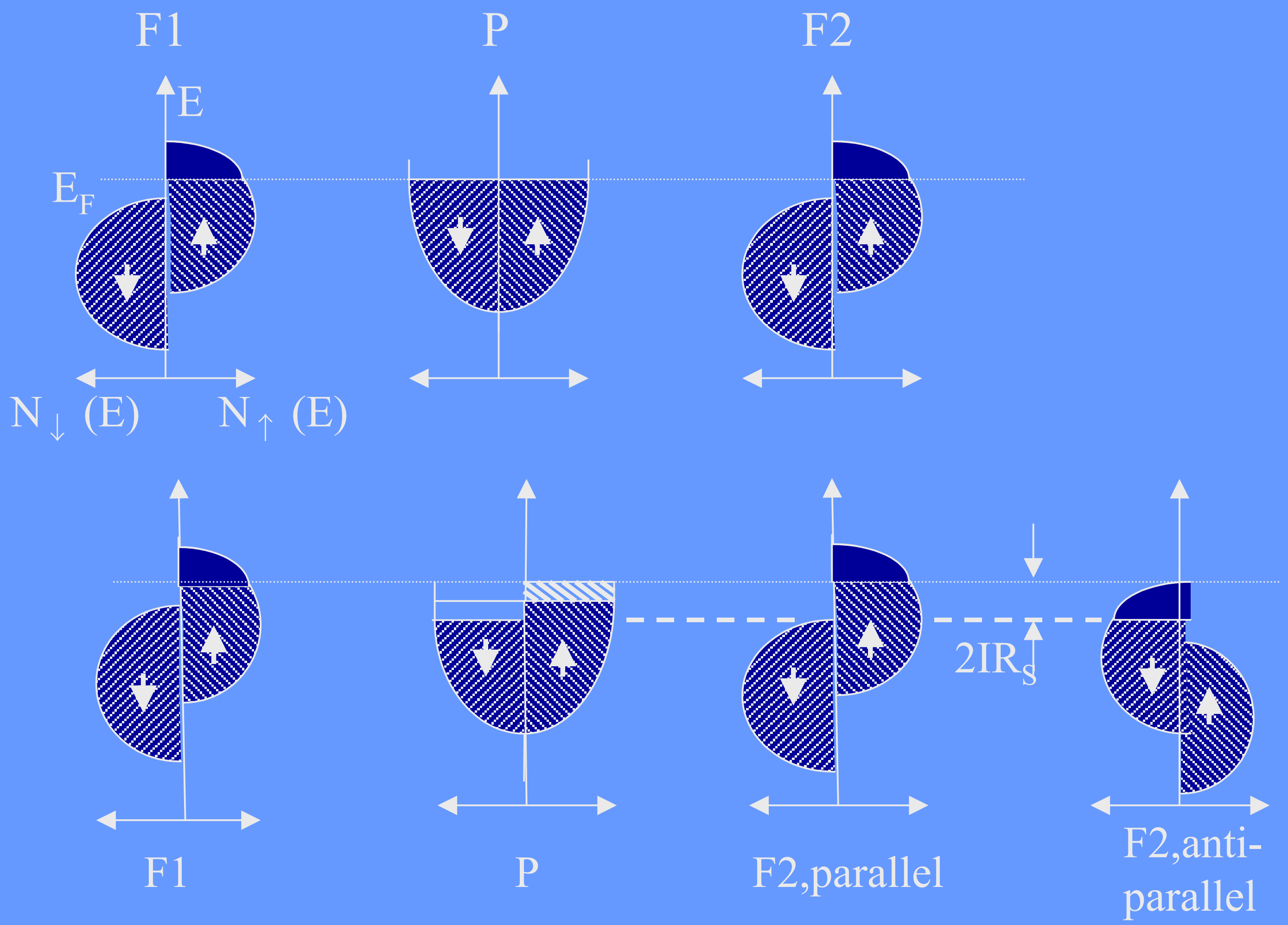

Fig. Model of the densities of states of two ferromagnetic films in interfacial contact with a paramagnetic film. **Top:** In equilibrium the Fermi levels align. **Bottom:** When a current is driven through the sandwich the voltage drop across the trilayers depends on the orientations of the magnetizations of the ferromagnetic films.

MR values as a function of metal content at R.T.

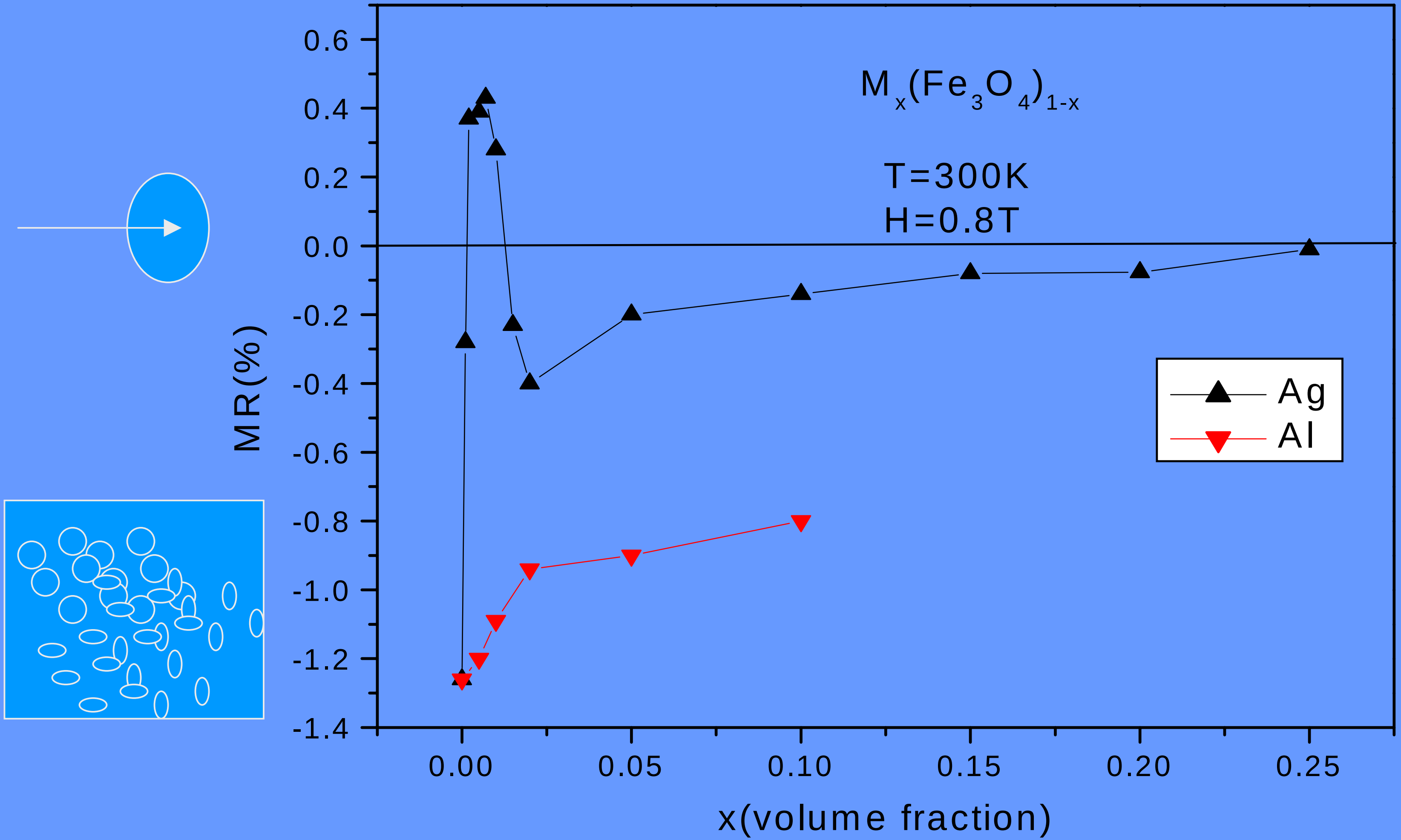

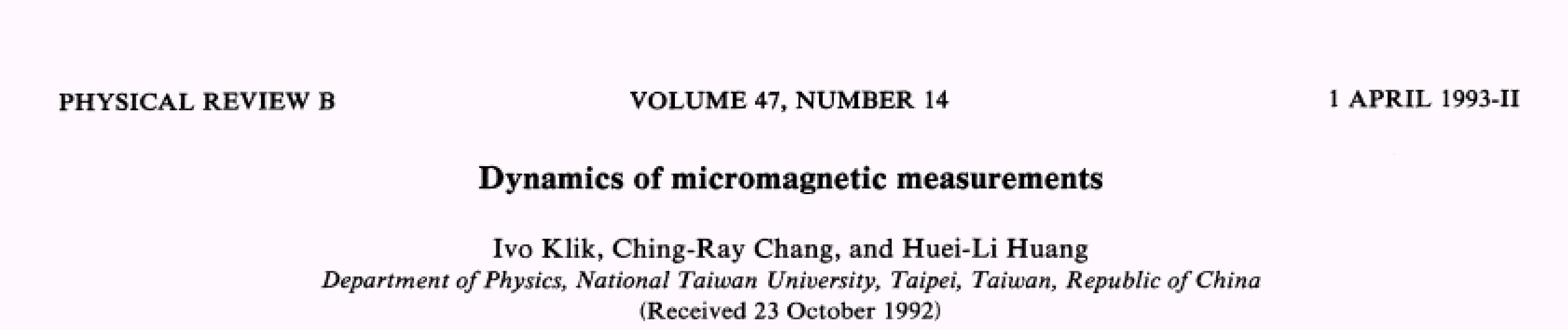
PHYSICAL REVIEW B VOLUME 47, NUMBER 14 1 APRIL 1993-II

Dynamics of micromagnetic measurements

Ivo Klik, Ching-Ray Chang, and Huei-Li Huang
Department of Physics, National Taiwan University, Taipei, Taiwan, Republic of China

(Received 23 October 1992)

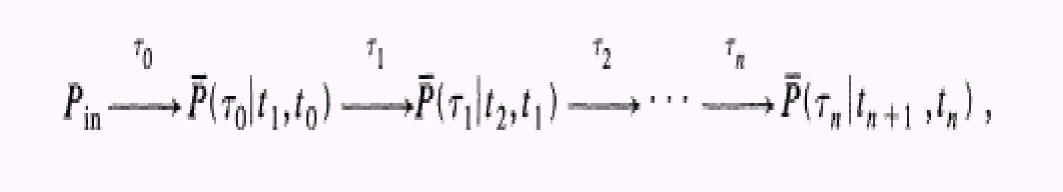

$$P_{\mathrm{in}} \xrightarrow{\tau_0} \bar{P}(\tau_0|t_1,t_0) \xrightarrow{\tau_1} \bar{P}(\tau_1|t_2,t_1) \xrightarrow{\tau_2} \cdots \xrightarrow{\tau_n} \bar{P}(\tau_n|t_{n+1},t_n)\,,$$

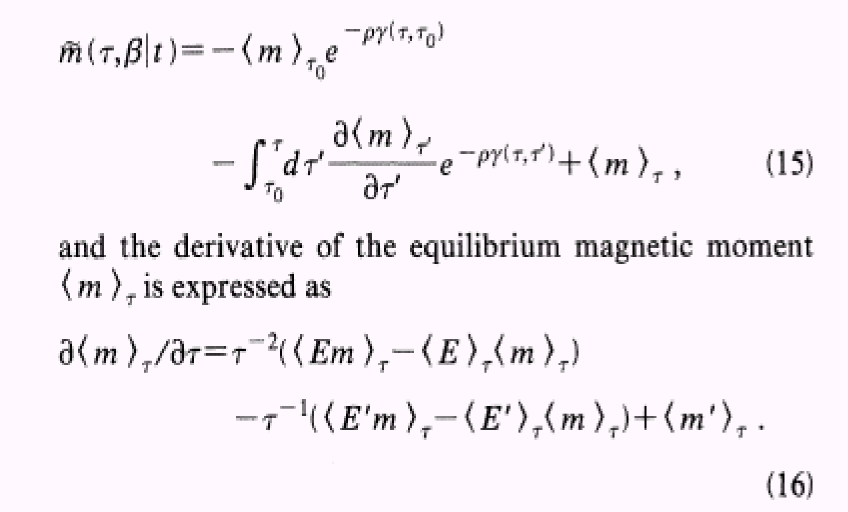

$$\tilde{m}(\tau,\beta|t) = -\langle m\rangle_{\tau_0} e^{-\rho\gamma(\tau,\tau_0)} - \int_{\tau_0}^{\tau} d\tau' \frac{\partial\langle m\rangle_{\tau'}}{\partial\tau'} e^{-\rho\gamma(\tau,\tau')} + \langle m\rangle_\tau\,, \qquad (15)$$

and the derivative of the equilibrium magnetic moment $\langle m\rangle_\tau$ is expressed as

$$\partial\langle m\rangle_\tau/\partial\tau = \tau^{-2}(\langle Em\rangle_\tau - \langle E\rangle_\tau\langle m\rangle_\tau) - \tau^{-1}(\langle E'm\rangle_\tau - \langle E'\rangle_\tau\langle m\rangle_\tau) + \langle m'\rangle_\tau\,. \qquad (16)$$

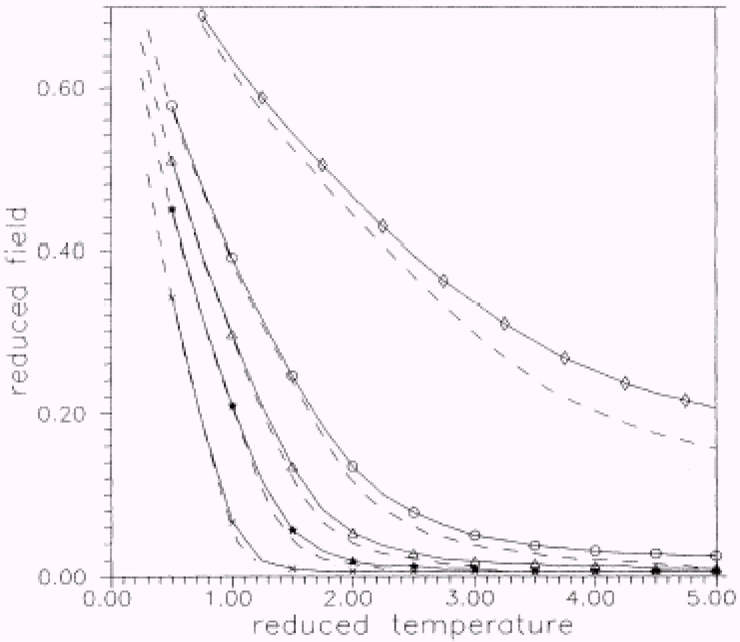

FIG. 1. The reduced coercivity $b_c = B_c(f,\vartheta)/B_N$ (solid lines) and the reduced field $b_\chi = B_\chi(f,\vartheta)/B_N$ (dashed lines) at which the susceptibility $\hat{\chi}[f,\vartheta|b,-1]$ has a maximum. The curves correspond to the sweep rates $f=10^2$ Hz (×), 10^4 Hz (✱), 10^5 Hz (△), 10^6 Hz (○), and 10^8 Hz (◇).

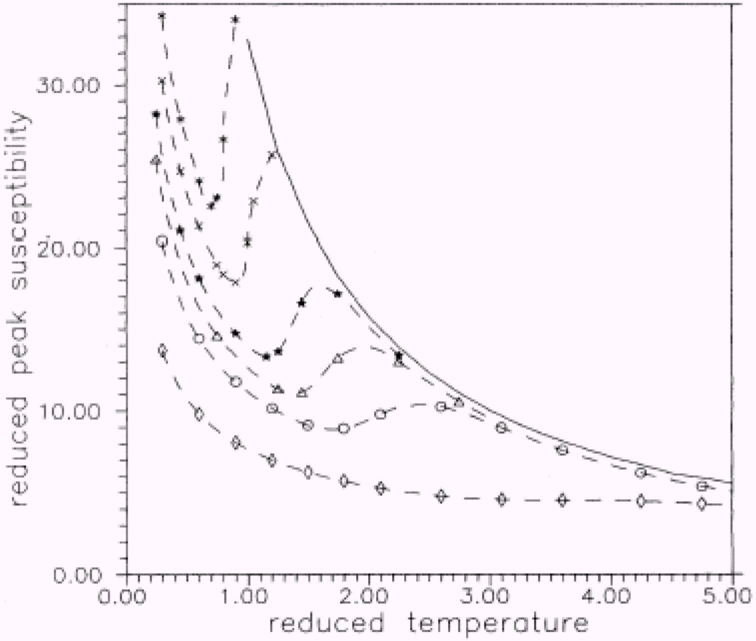

FIG. 5. The same peak values of reduced susceptibility as shown in Fig. 4, but plotted vs the reduced temperature ϑ. The solid line denotes equilibrium susceptibility $\chi_{\|}(\vartheta,0)$ at zero field. The tail section of the $f=10^0$- and 10^2-Hz curves could not be calculated with sufficient accuracy.

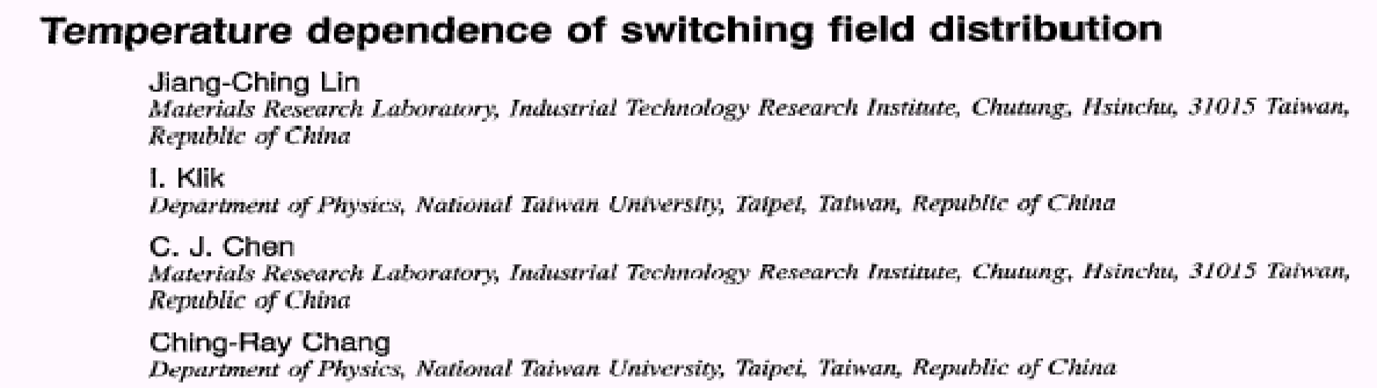

Temperature dependence of switching field distribution

Jiang-Ching Lin
Materials Research Laboratory, Industrial Technology Research Institute, Chutung, Hsinchu, 31015 Taiwan, Republic of China

I. Klik
Department of Physics, National Taiwan University, Taipei, Taiwan, Republic of China

C. J. Chen
Materials Research Laboratory, Industrial Technology Research Institute, Chutung, Hsinchu, 31015 Taiwan, Republic of China

Ching-Ray Chang
Department of Physics, National Taiwan University, Taipei, Taiwan, Republic of China

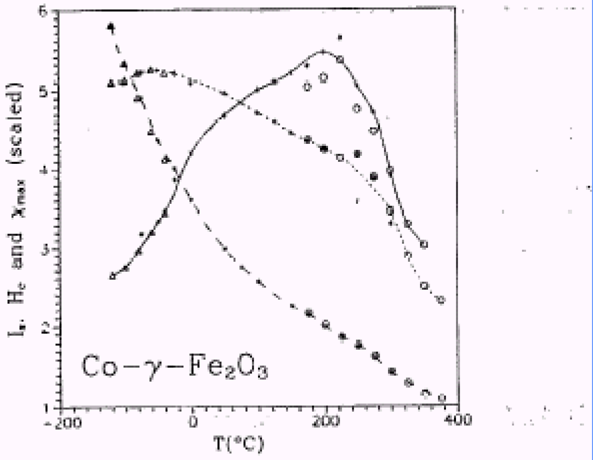

FIG. 1. Co-γ-Fe_2O_3 powder: Experimental dependence of the peak switching field distribution value χ_{max}, coercivity H_c and saturated magnetic moment I_s on temperature T. Units and markings: χ_{max} (arbitrary scale, full line), H_c (200 Oe, long dash), and I_s (arbitrary scale, short dash). The lines merely guide the eye. Three samples from the same production batch, distinguished by the symbols (O), (*), and (Δ).

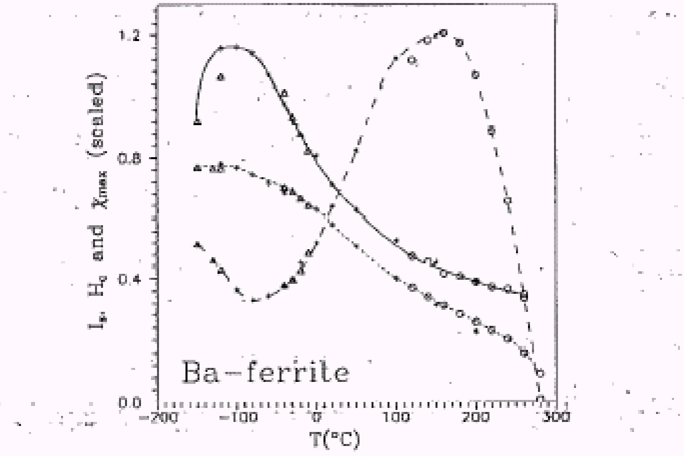

FIG. 3. Ba-ferrite platelets. Units and markings same as in Fig. 1 but with H_c (10^3 Oe). Three samples as in Fig. 1.

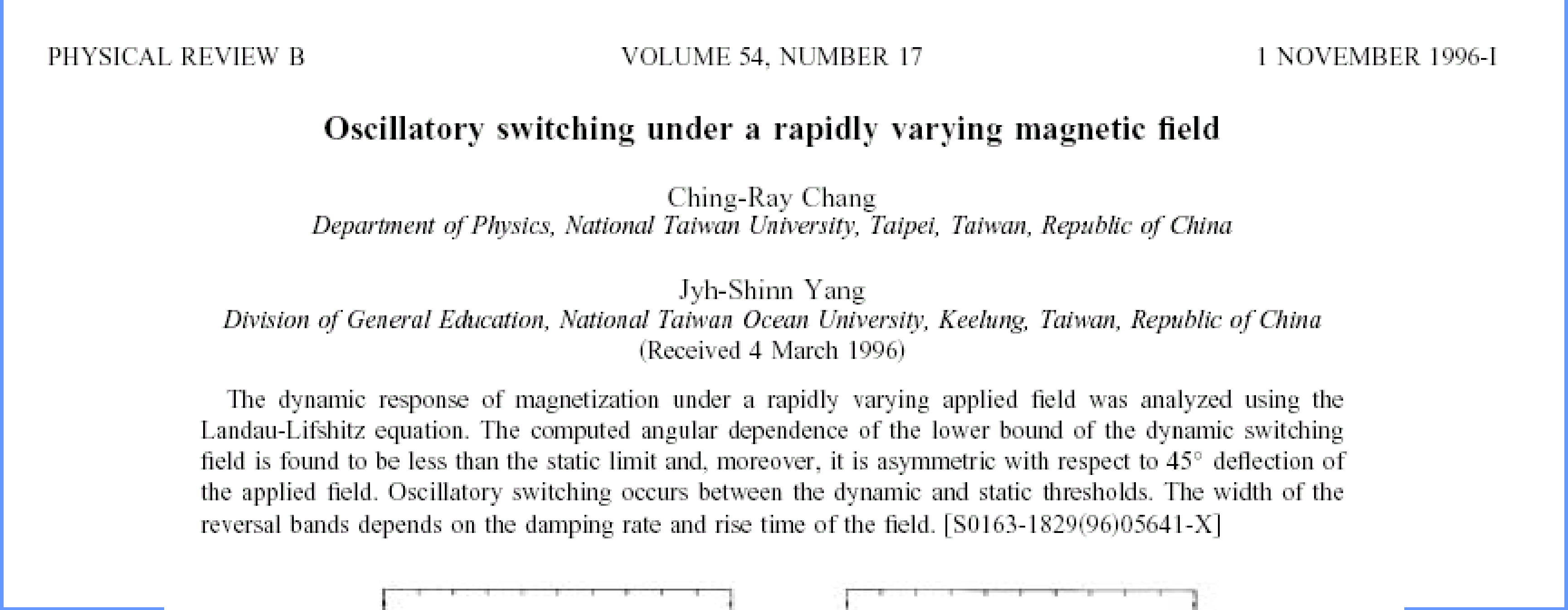

PHYSICAL REVIEW B VOLUME 54, NUMBER 17 1 NOVEMBER 1996-I

Oscillatory switching under a rapidly varying magnetic field

Ching-Ray Chang
Department of Physics, National Taiwan University, Taipei, Taiwan, Republic of China

Jyh-Shinn Yang
Division of General Education, National Taiwan Ocean University, Keelung, Taiwan, Republic of China

(Received 4 March 1996)

The dynamic response of magnetization under a rapidly varying applied field was analyzed using the Landau-Lifshitz equation. The computed angular dependence of the lower bound of the dynamic switching field is found to be less than the static limit and, moreover, it is asymmetric with respect to 45° deflection of the applied field. Oscillatory switching occurs between the dynamic and static thresholds. The width of the reversal bands depends on the damping rate and rise time of the field. [S0163-1829(96)05641-X]

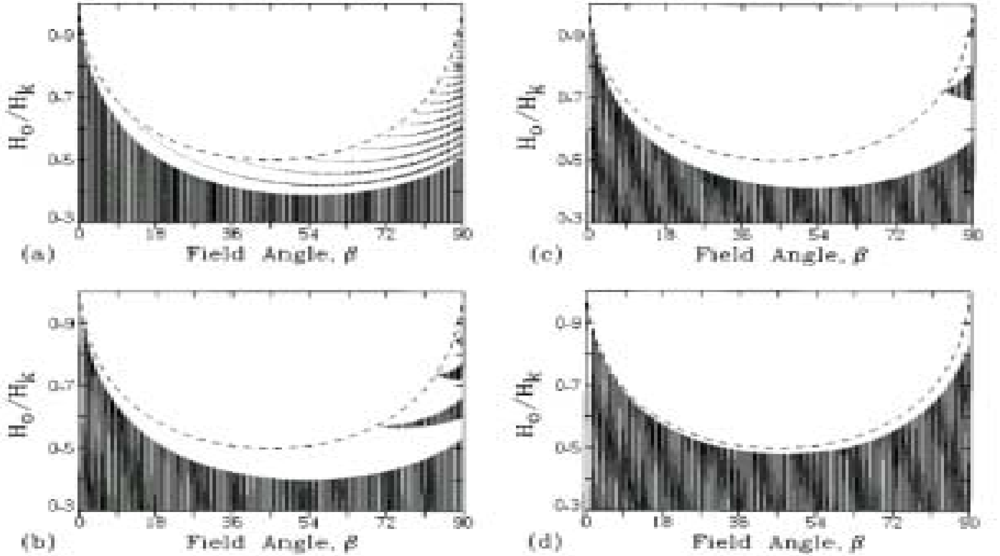

FIG. 2. Angular dependence of the switching field for stepwise applied field. Initial angle θ_i is along the easy axis and unshaded areas are the reversal regions. Dashed line is the Stoner-Wohlfarth limit. The rise time $\tau=0.1/\gamma H_k$ and damping constants α are 0.01 (a), 0.05 (b), 0.1 (c), and 0.5 (d), respectively.

TRFR

- Time-resolved Faraday rotation

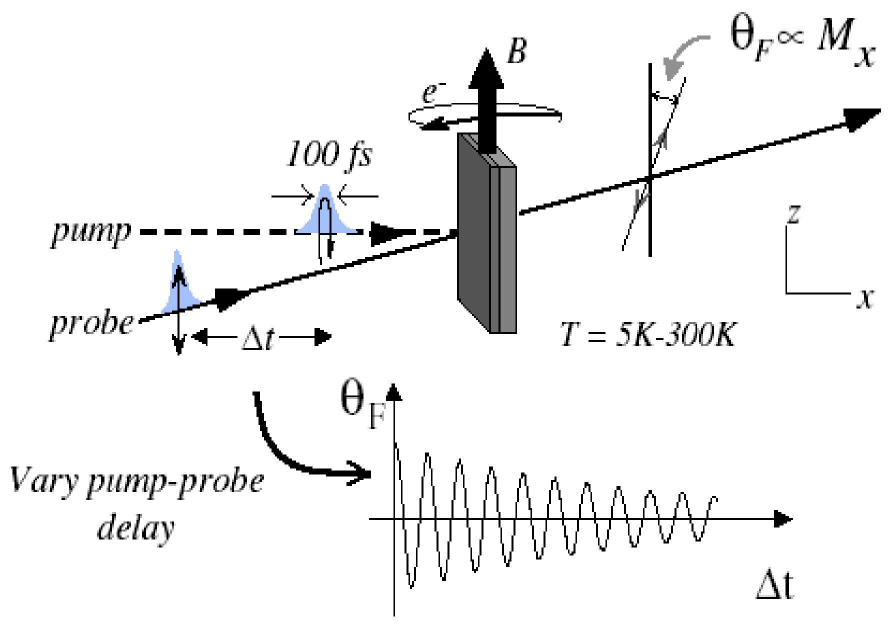

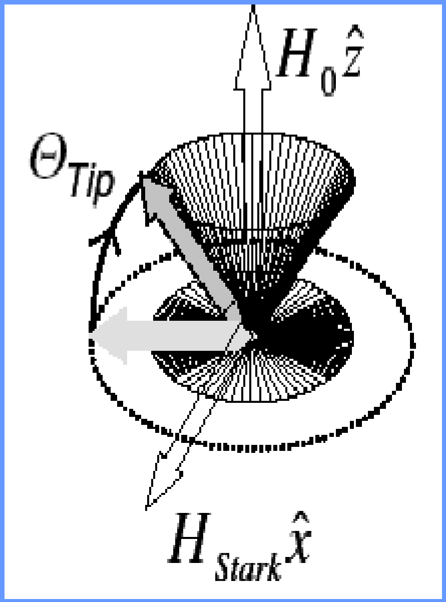

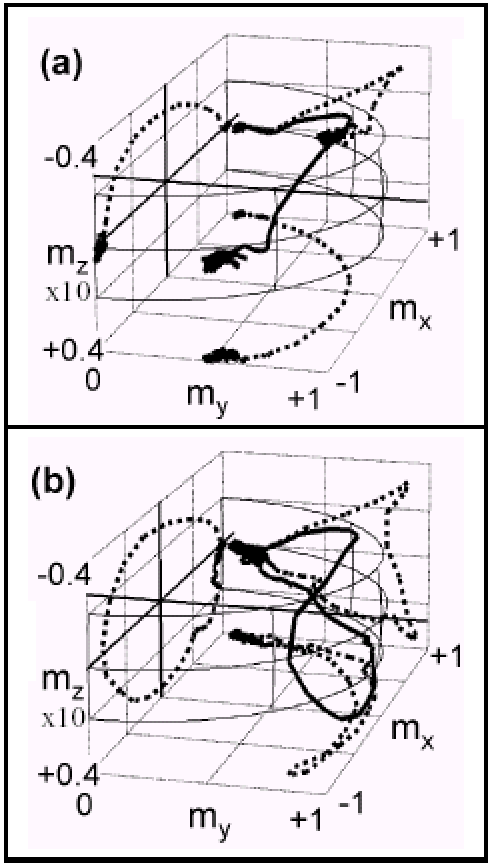

Fig. 1 Experimental data for 3D trajectory and projections of precessional magnetic switching.

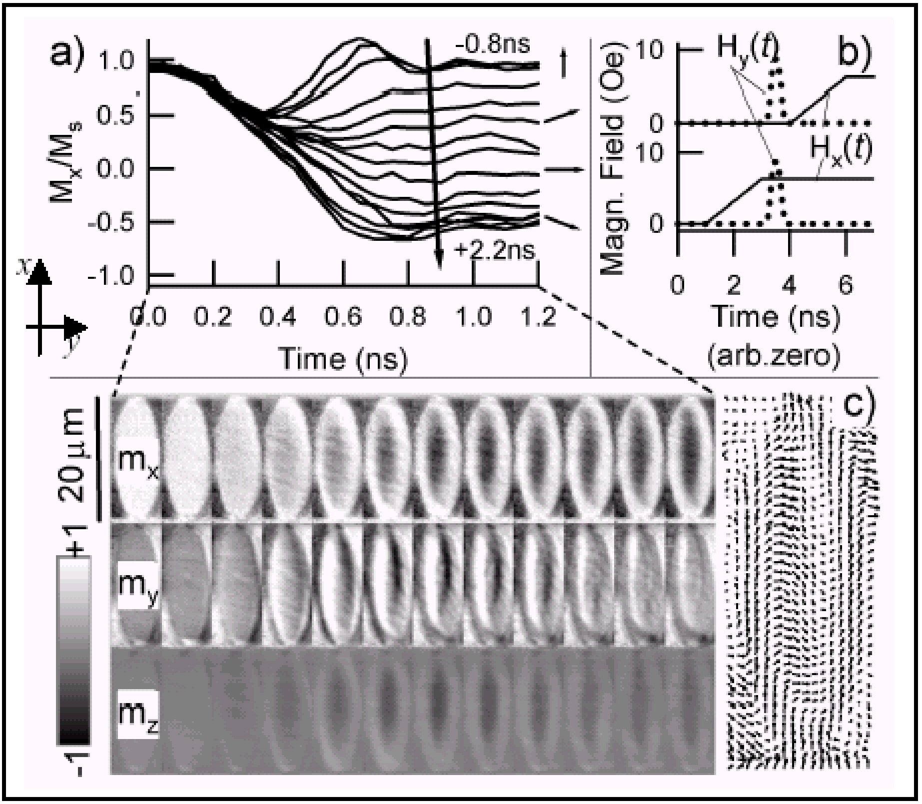

Fig. 2 Magnetization response to coincident orthogonal pulse fields. The overlap of $H_x(t)$ (6.3Oe and 15ns) and $H_y(t)$ (9Oe and 360ps), shown in **(b)** is a parameter in **(a)**. **(c)** Montage for the 2.2ns overlap (0.1ns steps) and vector image of last frame.

Ballistic Spin Transport across Ferromagnet/InAs(2DEG) Multi-junction Structures

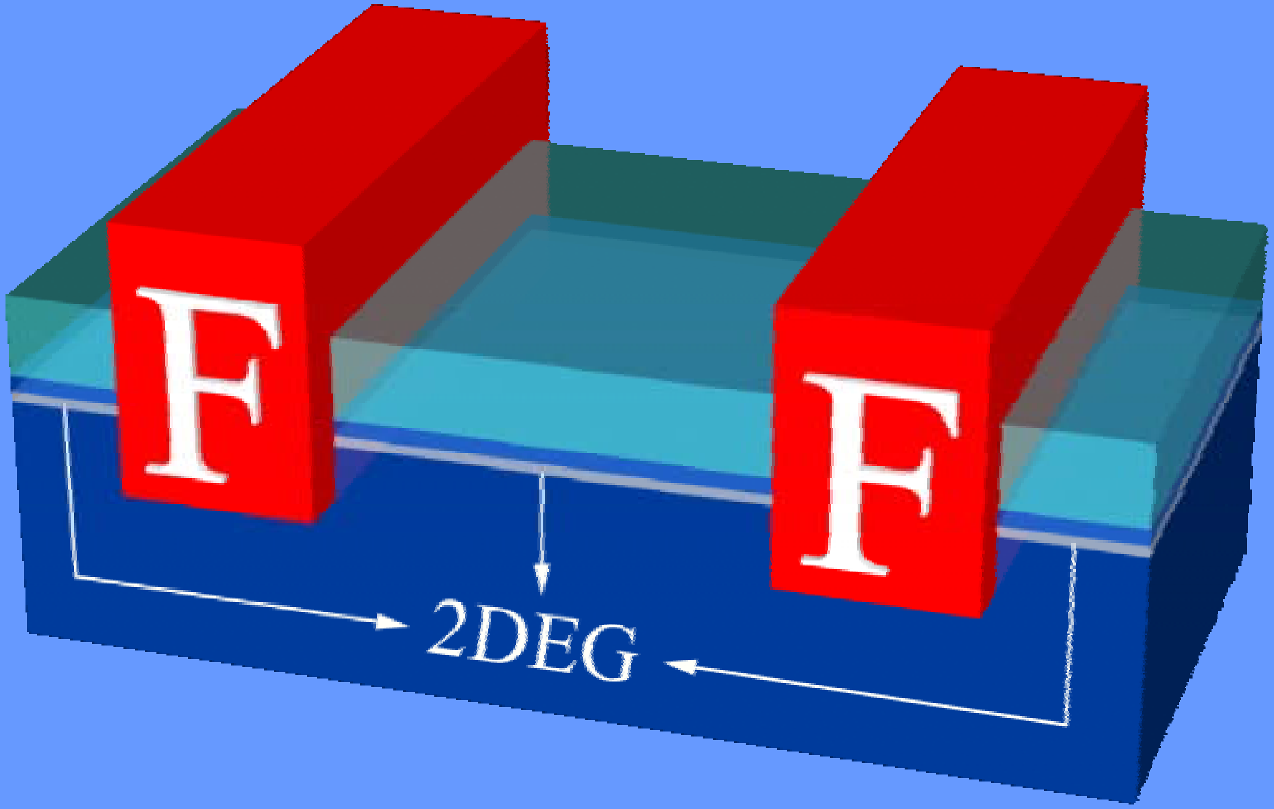

Rashba Spin Splitting

The effective magnetic field $\mathbf{B}_{eff}$ felt by a moving charge under an electric field:

the Rashba parameter

unit vector of surface electric field

$$H_R = \alpha[\boldsymbol{\sigma} \times \mathbf{k}] \cdot \mathbf{u}_\mathbf{E}$$

Pauli matrices in vector form

wave vector

Rashba Spin Splitting

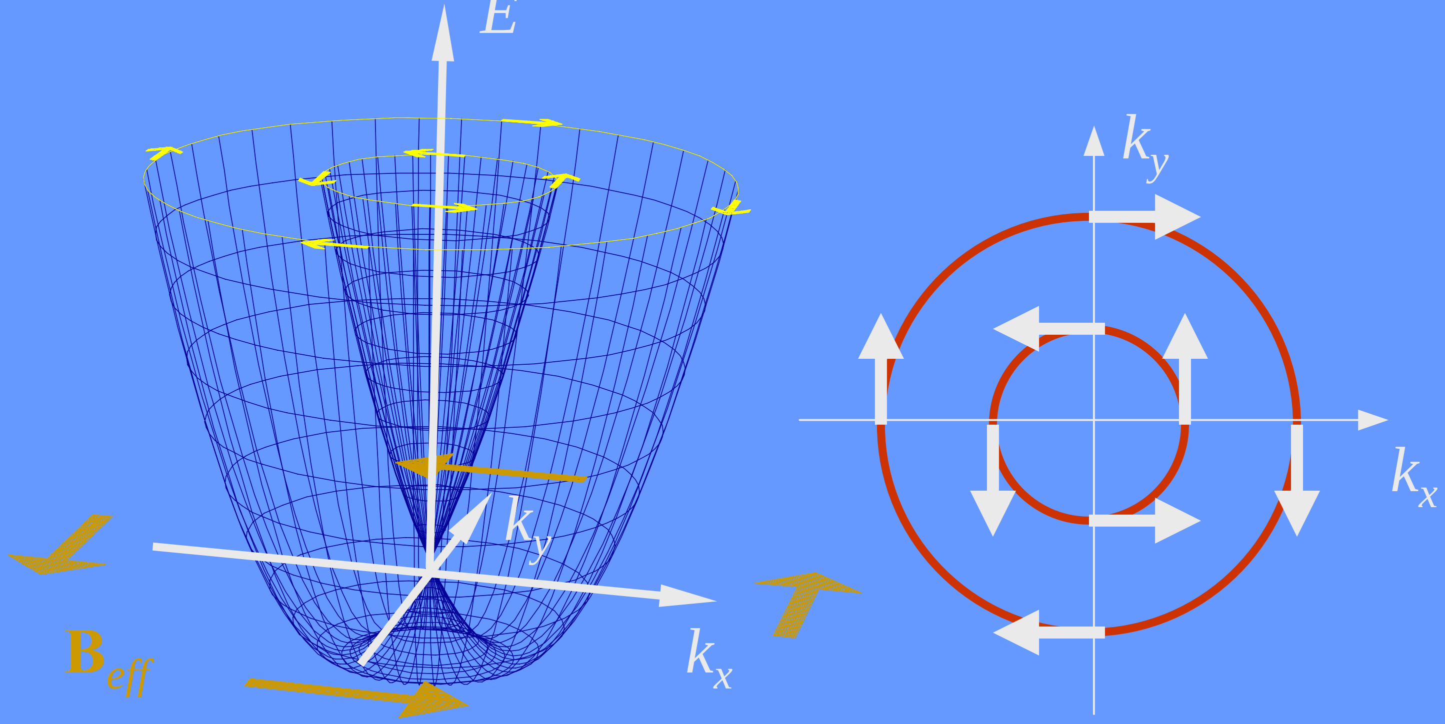

$$\mathbf{B}_{eff} = -\frac{1}{c}\mathbf{v}\times\mathbf{E}$$

磁性半導體分類

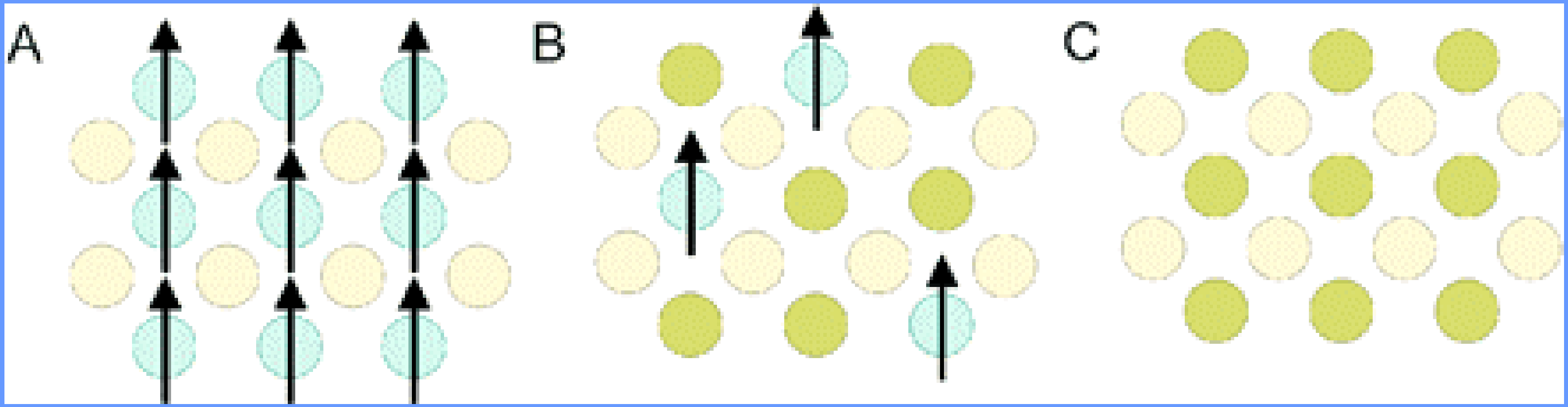

Three types of semiconductors: (A) a magnetic semiconductor, in which a periodic array of magnetic element is present; (B) a diluted magnetic semiconductor, an alloy between nonmagnetic semiconductor and magnetic element; and (C) a nonmagnetic semiconductor, which contains no magnetic ions. (From Ohno, Science 281, 951 (1998).)

MR H-R曲線與半導體 I-V曲線

半導體 I-V曲線：

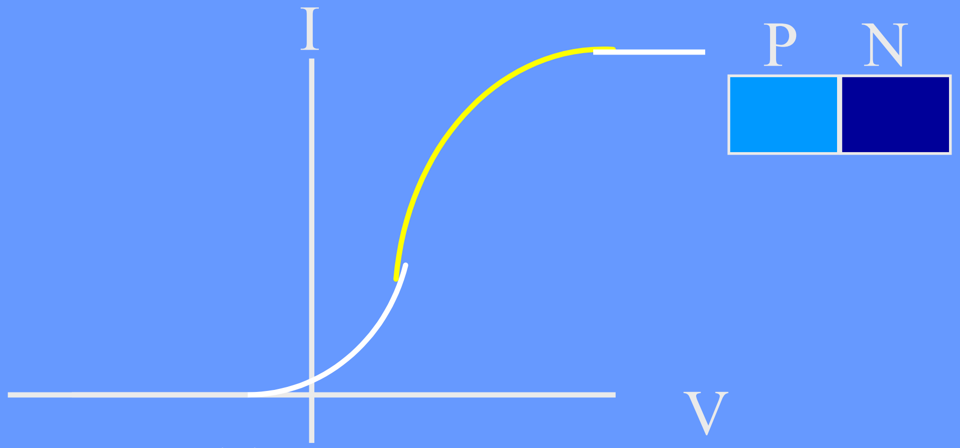

MR H-R曲線:

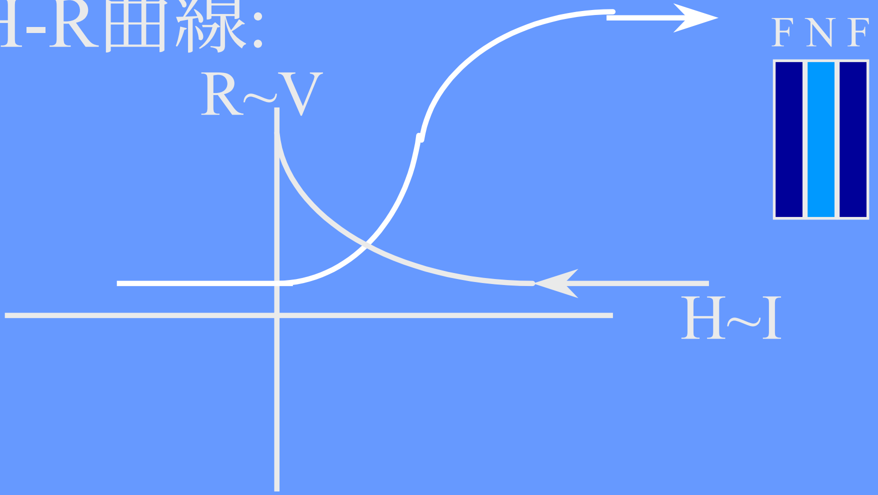

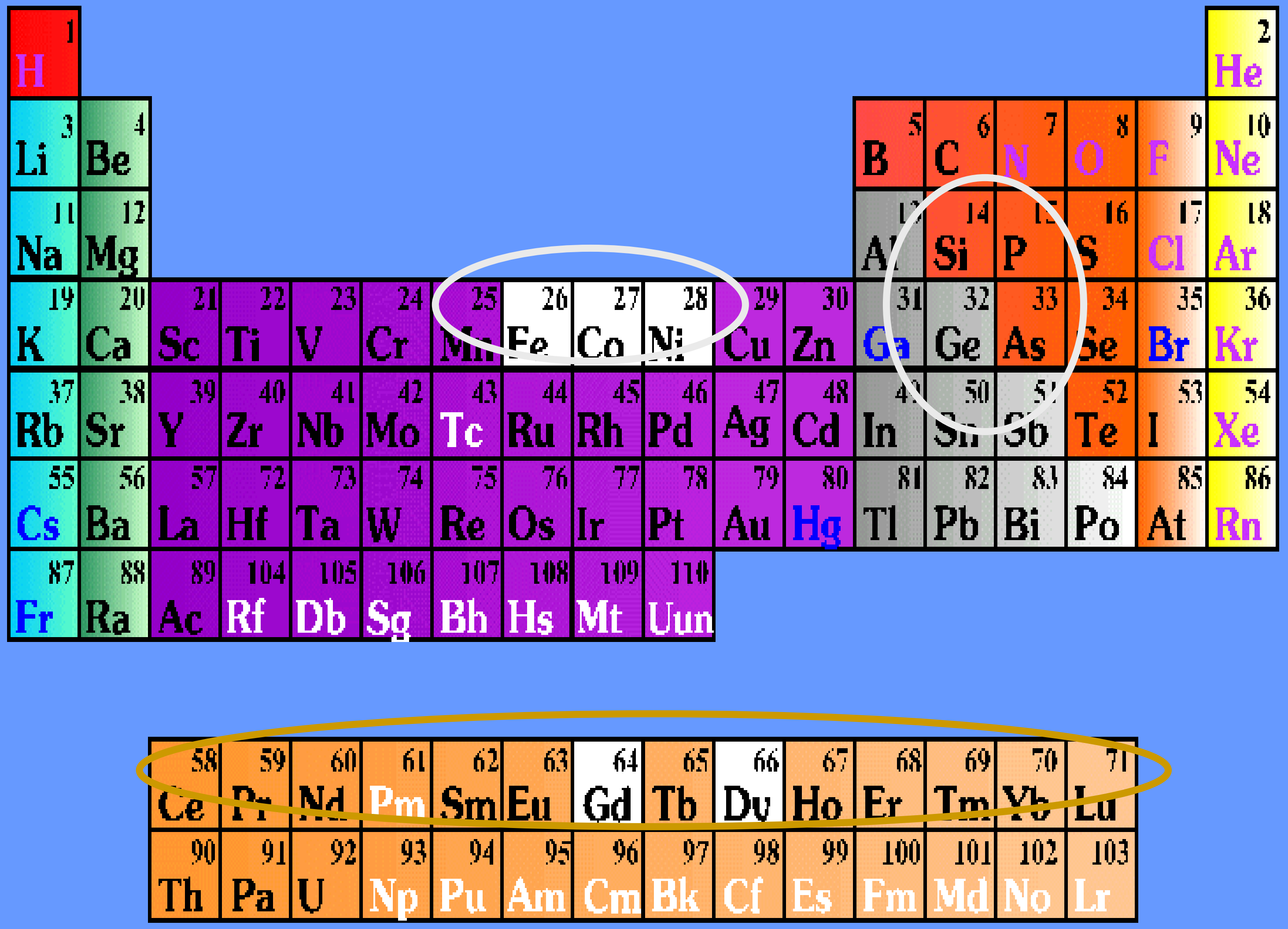

1 H																	2 He
3 Li	4 Be											5 B	6 C	7 N	8 O	9 F	10 Ne
11 Na	12 Mg											13 Al	14 Si	15 P	16 S	17 Cl	18 Ar
19 K	20 Ca	21 Sc	22 Ti	23 V	24 Cr	25 Mn	26 Fe	27 Co	28 Ni	29 Cu	30 Zn	31 Ga	32 Ge	33 As	34 Se	35 Br	36 Kr
37 Rb	38 Sr	39 Y	40 Zr	41 Nb	42 Mo	43 Tc	44 Ru	45 Rh	46 Pd	47 Ag	48 Cd	49 In	50 Sn	51 Sb	52 Te	53 I	54 Xe
55 Cs	56 Ba	57 La	72 Hf	73 Ta	74 W	75 Re	76 Os	77 Ir	78 Pt	79 Au	80 Hg	81 Tl	82 Pb	83 Bi	84 Po	85 At	86 Rn
87 Fr	88 Ra	89 Ac	104 Rf	105 Db	106 Sg	107 Bh	108 Hs	109 Mt	110 Uun								
		58 Ce	59 Pr	60 Nd	61 Pm	62 Sm	63 Eu	64 Gd	65 Tb	66 Dy	67 Ho	68 Er	69 Tm	70 Yb	71 Lu		
		90 Th	91 Pa	92 U	93 Np	94 Pu	95 Am	96 Cm	97 Bk	98 Cf	99 Es	100 Fm	101 Md	102 No	103 Lr		

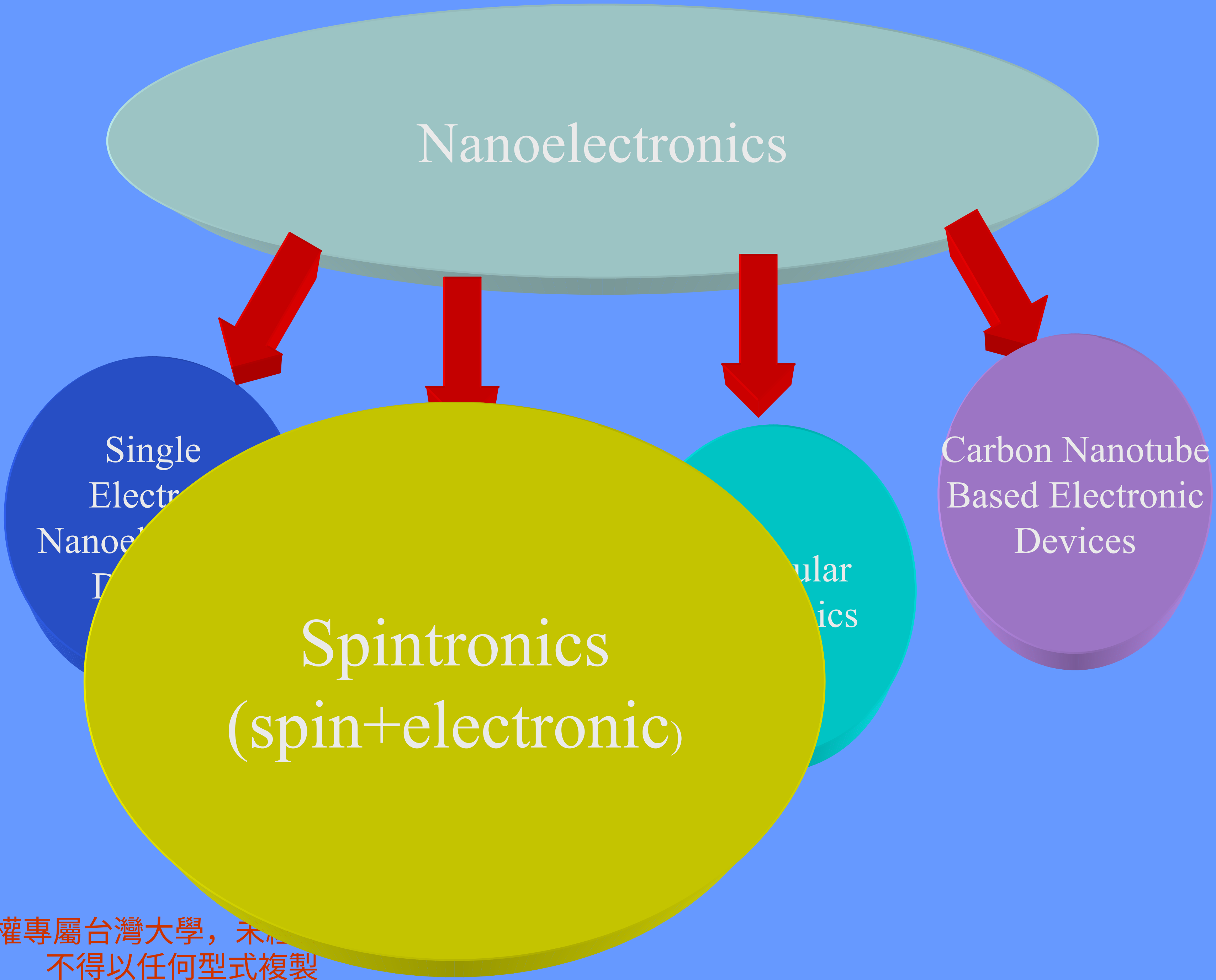

Nanoelectronics

Single
Electr
Nanoel
D

ular
ics

Carbon Nanotube
Based Electronic
Devices

Spintronics
(spin+electronic)

Applications of Spintronics

- Conventional MR—Existing
- Sensor and Reading Head—Existing
- **Spin transistor—New**
- **MRAM—New**
- **Magnetic logic device, quantum computer --New**

Areal Density of Magnetic HDD

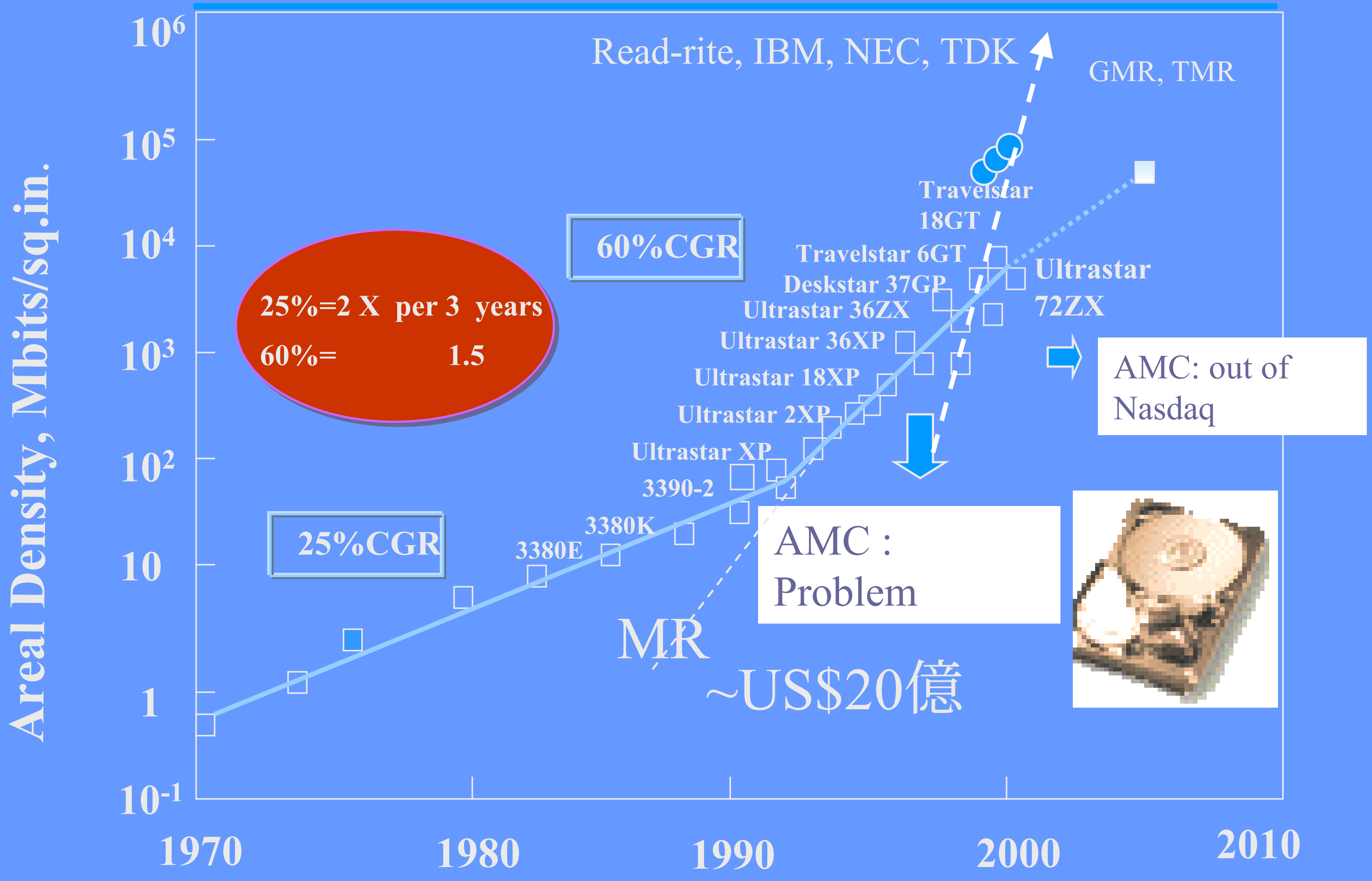

25%=2 X per 3 years

60%= 1.5

AMC: out of Nasdaq

AMC : Problem

~US$20億

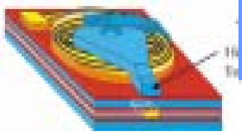

APPLIED MAGNETICS (Monthly Chart)

Perspectives of MRAM: Holy Grail

TMR MRAM Promises

High density of DRAM

High speed of SRAM

Non-volatility of FRAM

Low cost memory

Radiation Hard

Non destructive read-out

High speed, low power, non-volatility, large density, and no moving parts

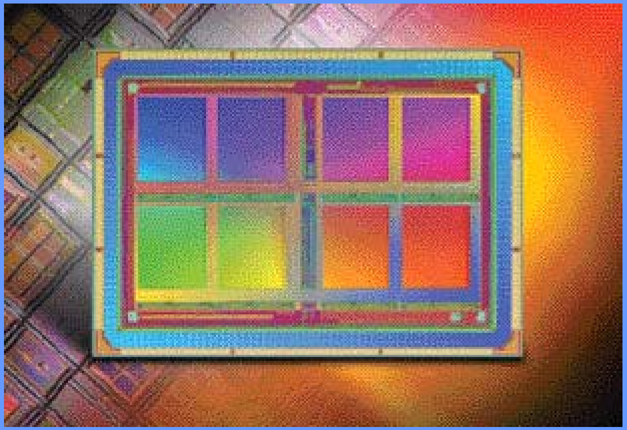

2003十月27日

摩托羅拉公司基於0.18微米技術的4Mb 的 MRAM晶片的推出是該行業的一條重大新聞。Honeywell 公司最近已批準將摩托羅拉的MRAM 技術用於軍用和航空航天應用產品。

→Growth Stage

FM/Conductors/FM

GMR : read head, sensors, MRAM

→ Developing Stage

FM/Insulators/FM

TMR : MRAM, read head, sensor

→ Fundamental Stage

FM/Semiconductors/FM

spin-polarized FET, Hall effect MRAM

→ Quickening Stage

FM /Superconductors/FM

New millenarian of Spintronics

Silicon Age

Silicon-Iron age ?